Geological Society of America Bulletin

Paleocene–Eocene syncontractional sedimentation in narrow, lacustrine-dominated basins of east-central Tibet

Brian K. Horton, An Yin, Matthew S. Spurlin, Jiangyu Zhou and Jianghai Wang

Email alerting services	click www.gsapubs.org/cgi/alerts to receive free e-mail alerts when new articles cite this article
Subscribe	click www.gsapubs.org/subscriptions/ to subscribe to Geological Society of America Bulletin
Permission request	click http://www.geosociety.org/pubs/copyrt.htm#gsa to contact GSA

Notes

THE
GEOLOGICAL
SOCIETY
OF AMERICA

Paleocene–Eocene syncontractional sedimentation in narrow, lacustrine-dominated basins of east-central Tibet

Brian K. Horton*
An Yin
Matthew S. Spurlin
Department of Earth and Space Sciences, University of California, Los Angeles, California 90095, USA

Jiangyu Zhou
Jianghai Wang
Guangzhou Institute of Geochemistry, Chinese Academy of Sciences, Guangzhou, China

ABSTRACT

Sedimentologic, stratigraphic, compositional, and structural data from four elongate basins (<15 km wide, >30 km long) in the Nangqian-Yushu region of east-central Tibet (near the headwaters of the Mekong and Yangtze Rivers) indicate nonmarine sedimentation synchronous with Paleocene–Eocene northeast-southwest shortening. Sedimentation in the Nangqian, Niuguoda, Xialaxiu, and Shanglaxiu basins involved (1) mud and carbonate accumulation in offshore to nearshore lacustrine environments and (2) gravel and sand deposition in fan-delta to alluvial-fan environments localized near basin margins. Growth strata in both fine- and coarse-grained deposits, primarily in upper levels of basin fill, provide evidence for sedimentation contemporaneous with motion on fold-thrust structures. Provenance data collected from 25 measured stratigraphic sections, including >1500 paleocurrent measurements and >150 conglomerate compositional analyses, show that each basin was fed sediment from several directions by proximal source areas composed of Carboniferous–Triassic rocks. The source-area proximity and a stratigraphic variability among the basins suggest that each basin evolved independently and was filled by sediment derived from relatively small drainage networks (<10³ km²). Age control for basin fill is based on Paleogene fossils, 38–37 Ma $^{40}Ar/^{39}Ar$ ages from volcanic rocks interbedded with uppermost strata of the Nangqian basin, and 51–49 Ma $^{40}Ar/^{39}Ar$ ages from igneous rocks that intrude and unconformably overlie strata of the Shanglaxiu basin. Strata containing middle Cretaceous palynomorph and ostracod assemblages are present only locally in the lowermost part of the Nangqian basin. Although the tectonic setting for Cretaceous sedimentation is unclear, early Tertiary basin development was controlled by thin-skinned fold-thrust deformation. We interpret the narrow widths of Paleocene–Eocene basins to be a result of thrust spacing, which in turn may have been controlled by the depth to the décollement (~5 km deep according to our balanced cross section) from which imbricate thrusts ramped up through the Carboniferous–Triassic section. Sedimentologic and provenance evidence for internal drainage, limited unroofing, and relatively low average sediment-accumulation rates in these syncontractional, plateau-interior basins indicates generally small drainage systems, short main-stem rivers, shallow regional slopes, and limited denudation in east-central Tibet during early Tertiary time. Such geomorphic conditions, which are similar to the modern low-relief interior of the Tibetan plateau, suggest that the deeply incised Mekong and Yangtze Rivers of eastern Tibet were not established until after the termination of Paleogene basin development in the region.

Keywords: Asia, basin, China, fold-thrust belts, plateaus, Tibet.

INTRODUCTION

Studies of foreland basins on the periphery of the Himalayan-Tibetan orogen have provided constraints on the depositional systems, erosional unroofing patterns, and kinematic histories of fold-thrust systems along the margins of the orogen (Bally et al., 1986; Graham et al., 1993; Song and Wang, 1993; Chen et al., 1995; Burbank et al., 1996; Sobel and Dumitru, 1997; DeCelles et al., 1998; Métivier et al., 1998). In contrast, sedimentary basins in the remote interior of the Tibetan plateau (Fig. 1) have received considerably less attention (Leeder et al., 1988; Burke and Lucas, 1989; Liu and Wang, 2001; Liu et al., 2001). These plateau-interior basins are important because they have the potential to provide information on not only the erosional and depositional processes that mitigate regional denudation and relief production, but also the structural processes that control, in part, crustal thickening and surface uplift. Systematic analyses of Cretaceous–Tertiary accumulations in Tibet may help resolve the history of erosion and deformation across the plateau prior to and during the India-Asia collision. These deposits also present a unique opportunity to evaluate the rates and styles of ancient geomorphic processes operating on local to regional scales—properties that can be directly compared to the low-relief, internal-drainage conditions in central and western Tibet and the deeply incised, major river systems in eastern Tibet (the Yellow, Yangtze, Mekong, Salween, and Tsangpo Rivers; Fig. 1).

The objective of this paper is to document the early Tertiary history of sedimentation and related contraction in the Nangqian-Yushu re-
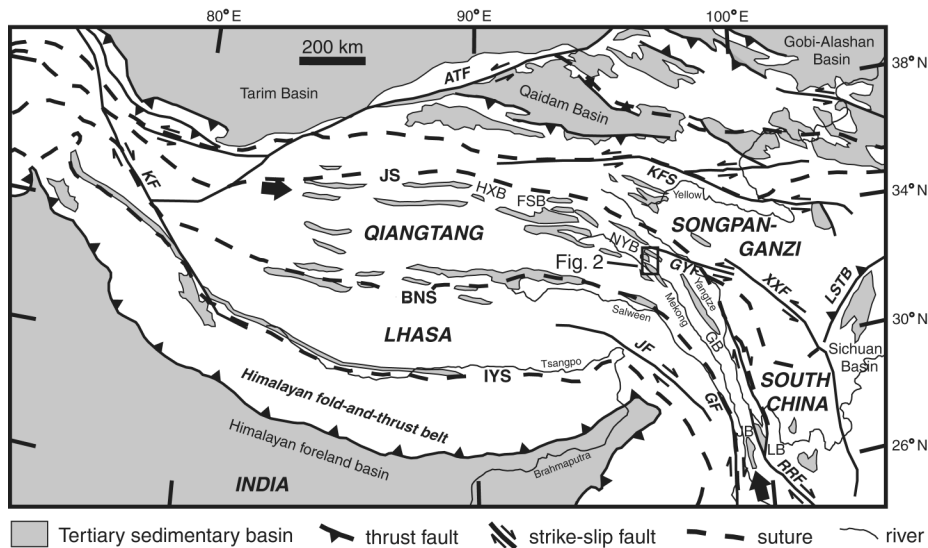
*E-mail: horton@ess.ucla.edu.

Figure 1. Simplified tectonic map of the Tibetan plateau, including sedimentary basins, faults, suture zones, and rivers (modified from Yin and Harrison, 2000). Shaded areas represent Cenozoic nonmarine deposits, including a belt of basins (denoted by arrows) that stretches from north-central Tibet (HXB—Hoh Xil basin; FSB—Fenghuo Shan basins) to east-central Tibet (NYB—Nangqian-Yushu basins) to southeastern Tibet and Yunnan province, south China (GB—Gongjue basin; LB—Lijian basin; JB—Jinggu basin). Also shown are sutures (JS—Jinsha suture; BNS—Bangong-Nujiang suture; IYS—Indus-Yalu suture) and major faults (KF—Karakorum fault; ATF—Altyn Tagh fault; KFS—Kunlun fault system; GYF—Ganzi-Yushu fault; XXF—Xiangshuihe-Xiaojiang fault system; LSTB—Longmen Shan thrust belt; RRF—Red River fault; GF—Gaoligong fault; JF—Jiali fault). Rectangular outline shows location of Nangqian-Yushu study region (Fig. 2).

gion of east-central Tibet (Fig. 2) in order to better understand the structural and geomorphic processes that helped build this part of the plateau. The four basins studied here may be broadly representative of the geomorphology, denudation patterns, and drainage systems of other basins in the plateau interior. In this respect, our analysis should serve as a baseline for further investigation of plateau-interior basins across Tibet and for comparison with better-studied foreland basins along the margins of the Himalayan-Tibetan orogen.

REGIONAL GEOLOGY

An arcuate, nearly continuous belt of mainly Paleogene rocks spans a distance of ~2000 km, from north-central Tibet through southeastern Tibet to Yunnan province, south China (Fig. 1) (Liu, 1988). This belt is associated with Tertiary thrusts in the west and strike-slip and transpressional fault systems in the east (Yin and Harrison, 2000; Wang et al., 2001). From west-northwest to east-southeast, the belt includes basins of the Hoh Xil, Fenghuo Shan, Nangqian-Yushu, and southeastern Tibet to south China regions. These basins oc-

cur along the northern part of the Qiangtang terrane (Fig. 1). The Qiangtang terrane is bounded by the Jinsha suture to the north, which represents latest Triassic collision with Triassic flysch of the Songpan-Ganzi terrane, and the Bangong-Nujiang suture to the south, which recorded Late Jurassic–Early Cretaceous collision with the Lhasa block (Allègre et al., 1984; Dewey et al., 1988; Nie et al., 1994; Metcalfe, 1996; Şengör and Natal'in, 1996; Yin and Nie, 1996; Zhou and Graham, 1996). Subsequent deformation along these and other suture zones during the India-Asia collision resulted in substantial Tertiary shortening and strike-slip faulting (Meyer et al., 1998; Yin and Harrison, 2000). Wang et al. (2001) have noted that lower Tertiary basins in eastern Tibet are spatially and temporally associated with arc-type igneous activity, leading them to suggest that the region may have been dominated by continental subduction during the early stage of the India-Asia collision. Most Neogene-Quaternary deformation in eastern Tibet apparently has been focused along regionally extensive strike-slip faults (Fig. 1) such as the left-lateral Kunlun, Xiangshuihe-Xiaojiang, and Ganzi-Yushu fault sys-

tems, the right-lateral Jiali-Gaoligong fault system, and the northern continuation of the currently right-lateral Red River fault (Armijo et al., 1989; Leloup et al., 1995; Van der Woerd et al., 2000; Wang and Burchfiel, 2000; Xu and Kamp, 2000). Although a few tens of kilometers of Neogene shortening occurred along the eastern edge of the plateau in the Longmen Shan thrust belt, this shortening appears insufficient to account for the thick crust and high elevation of the region (Burchfiel et al., 1995).

In the ~10^4 km² Nangqian-Yushu region (Fig. 2), lithologic units consist of Carboniferous–Triassic marine carbonates and minor clastic units overlain by a nonmarine succession of red clastic strata that has been assigned Jurassic, Cretaceous, and Paleogene ages (Liu, 1988; Qinghai BGMR, 1991). Minor Mesozoic and Tertiary intrusions have been mapped in the region, and the upper Paleogene interval locally contains interbedded volcanic rocks (Qinghai BGMR, 1991). The exposed upper Paleozoic through Cenozoic rocks could be underlain by Mesozoic accretionary melange, similar to the western Qiangtang terrane (Kapp et al., 2000), or by Middle Proterozoic to Cambrian basement known from the Lhasa terrane (Dewey et al., 1988; Harris et al., 1988; Yin and Harrison, 2000) and Greater Himalayan rocks (DeCelles et al., 2000).

BASINS OF THE NANGQIAN-YUSHU REGION

Structural Framework

The Tertiary Nangqian thrust system lies in the eastern part of the Fenghuo Shan–Nangqian thrust belt (Yin and Harrison, 2000). Our study area covers a traverse across the southern part of this thrust belt between the cities of Yushu in the north and Nangqian in the south (Figs. 1 and 2). The principal structures are southwest- and northeast-directed thrusts that juxtapose Paleozoic–Mesozoic strata over Tertiary strata. Evidence for dip-slip motion on the thrust faults includes mapped cutoff relationships and kinematic indicators such as fault striations and subsidiary mesoscopic folds in both hanging-wall and footwall blocks (Spurlin et al., 2000). These data indicate a N40°–50°E shortening direction in present-day coordinates. Minimum slip estimates for individual thrust faults range from ~2 to 18 km. Structural analyses across the Nangqian-Yushu region require a minimum of ~50% shortening, based on 51 km of shortening along a 54-km-long profile (Fig. 2B) (Spurlin et al., 2000).
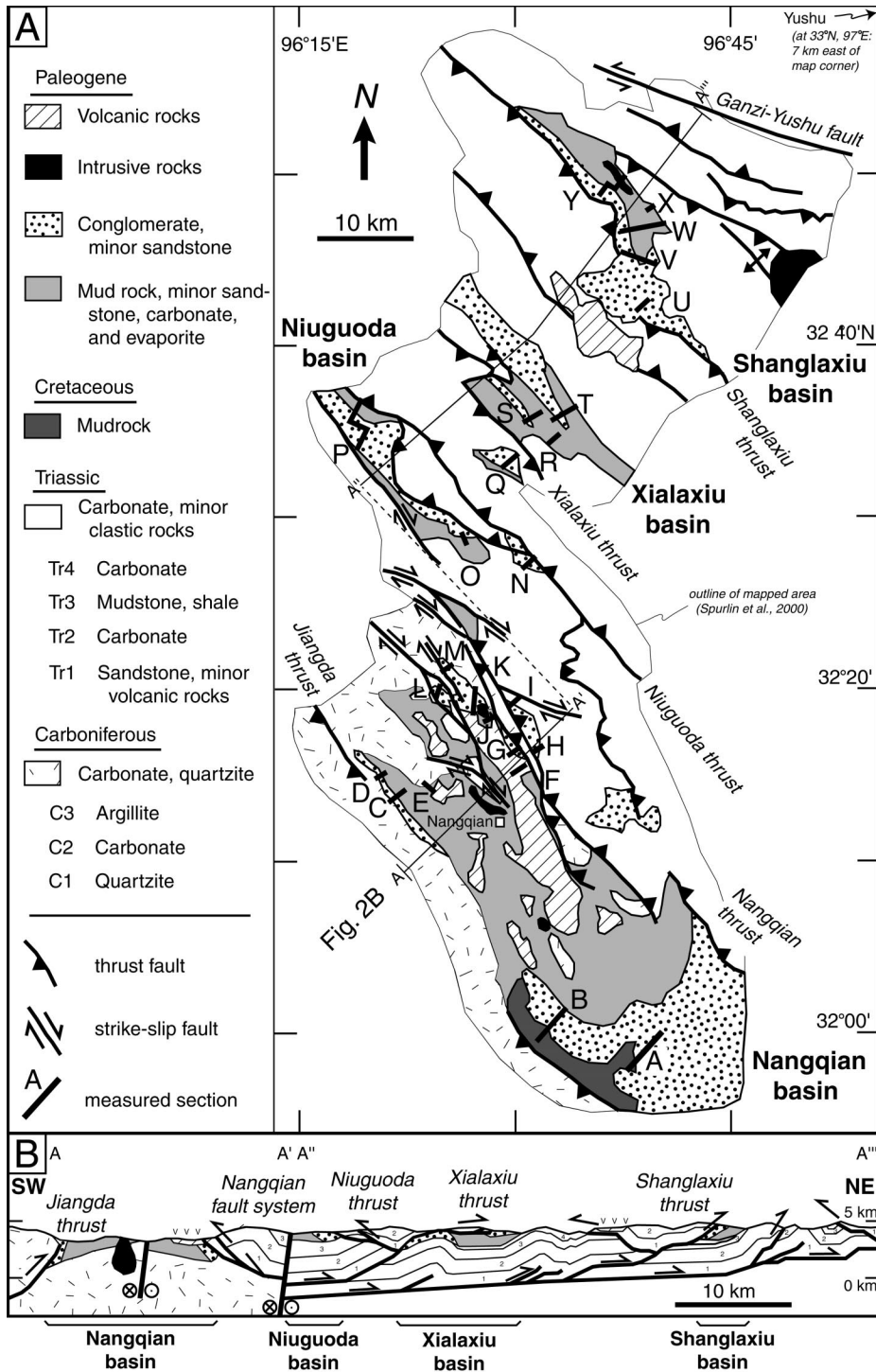
Figure 2. Generalized geologic map and cross section of the Nangqian-Yushu region (location shown in Fig. 1). (A) Map depicting structures and rock types of four Cretaceous–Paleogene outcrop belts and underlying Carboniferous–Triassic rocks, after Qinghai BGMR (1983a, 1983b) and Spurlin et al. (2000). Locations of 25 measured stratigraphic sections (sections A–Y) are shown. Basin fill includes primarily fine-grained deposits (shaded patterns). Coarse-grained deposits (random-dot pattern) are confined to margins of outcrop belts. (B) Cross section illustrating surface and inferred subsurface structural geometries. Basin dimensions are controlled by spacing of thin-skinned thrusts above an ~5-km-deep décollement. Numerals 1–4 refer to four Triassic units, and "V" pattern denotes Paleogene volcanic rocks. Simplified from Spurlin et al. (2000).

Right-slip faults cut the thrust faults, particularly along the northern margin of the Nangqian basin (Fig. 2). Estimates of right-lateral separation based on Carboniferous, Triassic, and Cretaceous–Paleogene marker units suggest a minimum of 15 km of cumulative right slip on these faults (Spurlin et al., 2000). The younger right-slip faults in the study area represent the northern termination of the Batang-Lijiang fault system (Wang et al., 2001), which is linked with the Red River fault to the south-southeast.

Stratigraphy

The Paleozoic and Mesozoic stratigraphy in the study area (Fig. 2) is dominated by three Carboniferous units (C1, quartzite; C2, carbonate; and C3, argillite) and four Triassic units (Tr1, sandstone; Tr2, carbonate; Tr3, mudstone; and Tr4, carbonate). In addition to fossil content (Qinghai BGMR, 1983a, 1983b, 1991), these units can be differentiated in the field on the basis of lithology, texture, bedding, and outcrop characteristics.

The four major outcrop belts of Cretaceous–Paleogene strata in the study region contain stratigraphic successions consisting of mudstone, sandstone, conglomerate, and minor carbonate and volcanic rocks (Fig. 3). Although early mapping studies (Qinghai BGMR, 1983a, 1983b) correlated stratigraphic units across all four outcrop belts, our field observations show that the generalized stratigraphic columns for each belt are sufficiently different (Fig. 3) to question such regional correlations. For example, localized coarse-grained facies are commonly confined to the margins of individual outcrop belts (Fig. 2), suggesting that these deposits were not regionally extensive and cannot be used to define a reliable regional lithostratigraphy. Nevertheless, because most successions exhibit a fining-upward pattern in which carbonate strata are limited to uppermost basin fill, we tentatively correlate the upper carbonate-bearing intervals among three of the four outcrop belts (Fig. 3). Although the carbonate intervals are not considered to represent a single regionally continuous lithostratigraphic unit, they may be age-equivalent strata (as suggested by similar reported fossils) that were deposited during a climatic phase conducive to carbonate precipitation. Paleogene fossils for all four basins include mollusks (*Hippeutis* sp., *Negulus* sp., *Cinima* sp., *Bithynia* sp.), pollen (*Pterisiporites* sp.), and plant fossils (*Clelmus* sp.) (Qinghai BGMR, 1983a, 1983b). According to our correlation scheme, a lack of carbonate in the Shanglaxiu basin suggests that the uppermost
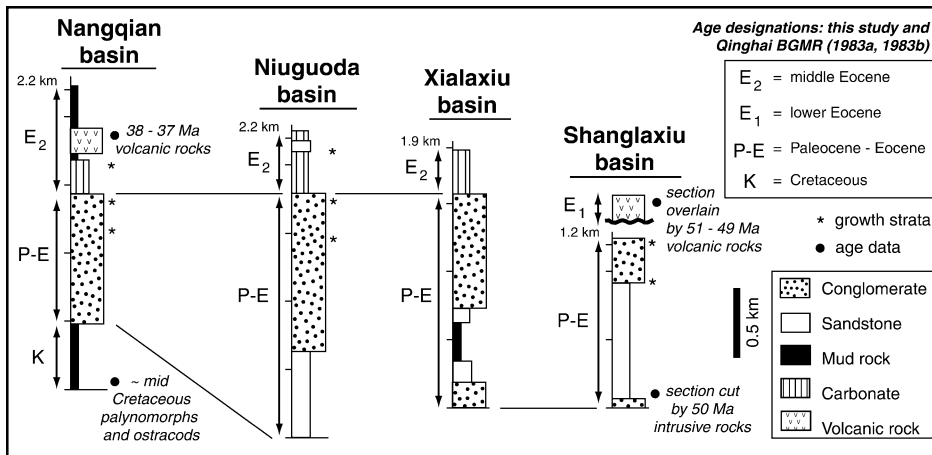
Figure 3. Composite stratigraphic columns, age constraints, and proposed stratigraphic correlations for the Nangqian-Yushu region. Lithologic depictions are generalized from measured sections (Fig. 4). New age constraints are provided by fossils (this study) and $^{40}Ar/^{39}Ar$ ages from tuffs and intrusions (Spurlin et al., 2000). Correlations are made on the basis of available age control and carbonate strata in uppermost basin fill (see text for discussion).

fill of this basin is older than that of the other basins. This interpretation is consistent with isotopic ages (discussed subsequently) for various Eocene volcanic rocks interbedded with the uppermost fill of the Nangqian basin yet unconformably overlying the uppermost fill of the Shanglaxiu basin (Fig. 3).

On the basis of 25 measured sections (Fig. 4)[1] we have identified differences in local lithofacies, paleocurrents, and conglomerate compositions among the four outcrop belts that indicate that each belt evolved as a separate basin. For this reason, we refer to the four belts as distinct basins: the Nangqian, Niuguoda, Xialaxiu, and Shanglaxiu basins, from south to north (Figs. 2 and 3). Within individual basins, correlations between measured sections (Fig. 4) are based on tracing of laterally continuous lithostratigraphic units over distances of a few kilometers and projection of beds along strike through areas of poor exposure.

New Age Control

Fossil Assemblages

Palynomorph and ostracod assemblages suggest an approximately middle Cretaceous age for the mudstone-dominated lowermost succession of the Nangqian basin in the southern part of the study area. Palynomorphs near the base of section A (Fig. 4) include *Chomotriletes fragilis*, *Distaltriangulisporites irre-*

gularis, *Gleicheniidites senonicus*, and *Podocarpidites epistratus*, which range throughout the Late Jurassic and Cretaceous. Absences of *Classopollis* (common to abundant in Late Jurassic and Early Cretaceous palynofloras) and angiosperm pollen (rare in late Albian but abundant in Late Cretaceous palynofloras) suggest the middle Cretaceous as the most probable age (e.g., Su et al., 1983). An ostracod assemblage from the lower part of section B (Fig. 4) is monotypic, exclusively represented by a species that belongs to the genus *Djungarica*, possibly the species *Djungarica solida* Jiang. Given only a single species, a precise age is difficult to assign. According to some authors, the genus *Djungarica* ranges throughout Late Jurassic and Early Cretaceous (Li and Yang, 1983; Li, 1988; Pang and Whatley, 1990). Ostracod fauna and poorly preserved charophyte oogonia from the same stratigraphic level attest to a lacustrine environment. The low ostracod diversity may suggest waters high in dissolved solutes.

Although the mudstone interval was originally mapped as the Upper Jurassic Yangshiping Formation (Qinghai BGMR, 1983a, 1991), age data for palynomorph and ostracod assemblages suggest approximately a middle Cretaceous age of deposition. These rocks represent the oldest known nonmarine deposits within any of the basins in the study region (Fig. 2). The organic-rich mudstone facies in this interval (described subsequently) is exclusively observed in mid-Cretaceous strata of the Nangqian basin (sections A and B in Fig. 4). We suggest, therefore, that middle Creta-

ceous sedimentation was limited to the Nangqian basin and that other basins recorded mainly Paleocene–Eocene deposition. Because the middle Cretaceous strata are located in the lowermost part of our measured sections (Fig. 4), the coarser-grained facies and syncontractional growth strata in middle to upper stratigraphic levels of the Nangqian basin must be younger than middle Cretaceous.

$^{40}Ar/^{39}Ar$ Geochronology

Spurlin et al. (2000) reported $^{40}Ar/^{39}Ar$ ages from tuffs interbedded with uppermost basin fill, volcanic rocks unconformably overlying basin fill, and intrusions that crosscut basin fill. Most ages are based on step-heating and total-fusion analyses of biotite separates. $^{40}Ar/^{39}Ar$ ages have been obtained for upper middle Eocene tuffs in the uppermost strata of the northern Nangqian basin (eight samples dated at 38.2 ± 0.1 Ma to 37.2 ± 0.1 Ma; sections E, F, H, I, and K in Fig. 4), upper middle Eocene intrusions cutting the intermediate to upper levels of the central and northern Nangqian basin (three samples dated at 37.7 ± 0.2 Ma to 37.0 ± 0.2 Ma; sections J–L in Fig. 4), lower Eocene volcanic rocks unconformably overlying the Shanglaxiu basin (two samples dated at 51.2 ± 0.2 Ma and 49.5 ± 0.2 Ma; capping section U in Fig. 4), and lower Eocene intrusions cutting the lower levels of the Shanglaxiu basin (one sample dated at 49.7 ± 0.2 Ma; section X in Fig. 4). For the Nangqian basin, these ages indicate final sediment accumulation in the basin during late middle Eocene time (Figs. 2 and 3). For the Shanglaxiu basin, lower Eocene intrusions and volcanic rocks postdate basin fill, providing a minimum age for Shanglaxiu basin development.

Growth Strata

Contractional growth-strata relationships are preserved within coarse-grained (Fig. 5, A and B) and fine-grained successions (Fig. 5, C and D) along several basin-margin structures and a few intrabasinal structures. The stratigraphic intervals containing growth strata (shown schematically in Fig. 3 and in detail in Fig. 4) are limited to the upper stratigraphic levels of the different basins. In each case, growth strata are characterized by an up-section decrease in bedding dip of 10°–90°, a notable decrease in bedding thickness (typically several tens of meters) toward the structure, and a common pattern of stratal onlap onto the margins of fault-related folds. These features indicate slip on thrust faults and progressive tilting (rotation) of fold limbs synchronous with sedimentation (e.g., Riba, 1976).

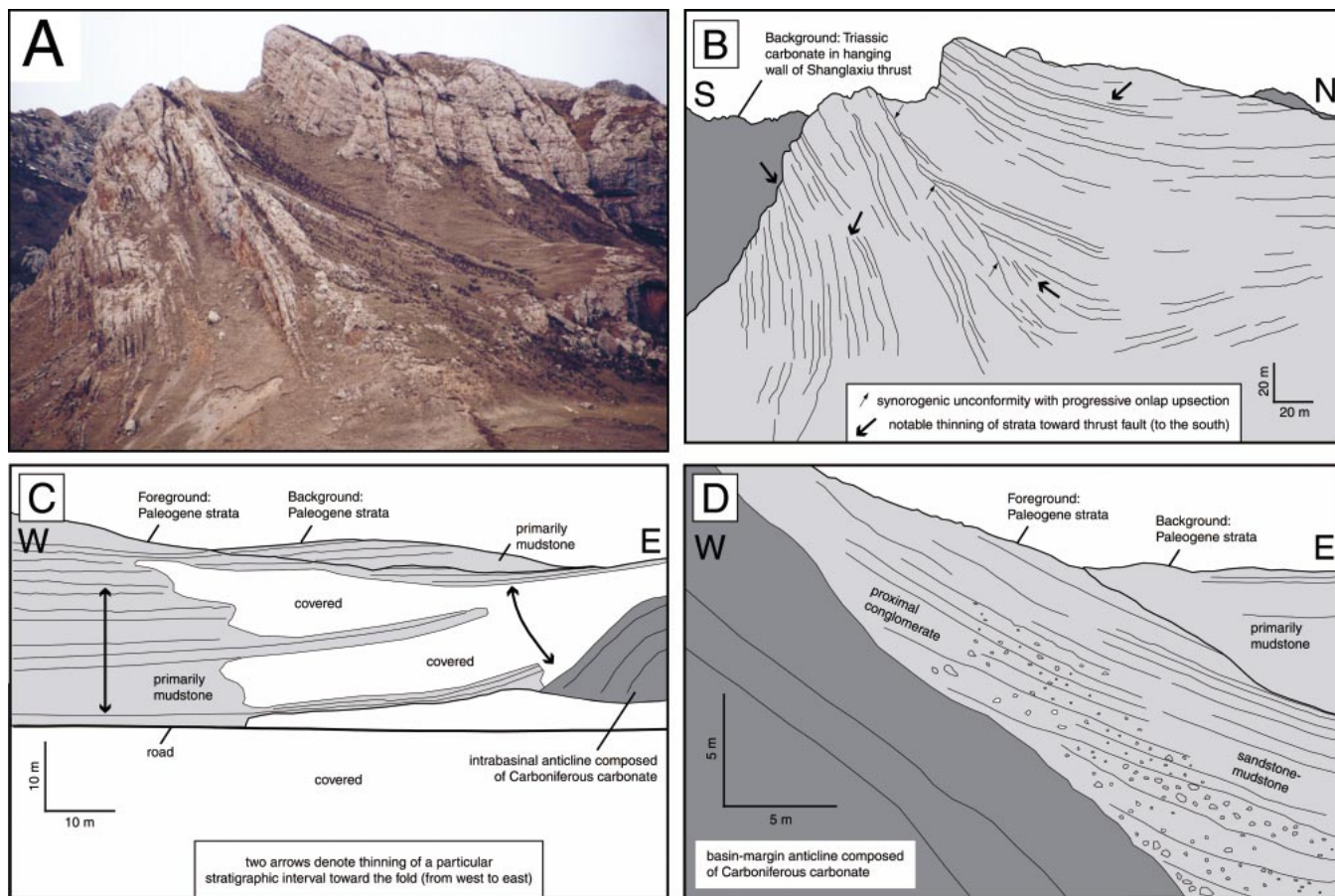[1]Figure 4 is on a separate sheet accompanying this issue.

Figure 5. Growth-strata successions and stratigraphic geometries along fold-thrust structures in the Nangqian-Yushu region. (A) Photograph and (B) line drawing of a conglomeratic growth syncline in the footwall of the north-directed Shanglaxiu thrust, northern Shanglaxiu basin, section Y (Figs. 2 and 4). Note the thinning of beds to the south (left), southward stratal onlap relationship (small arrows), and progressive up-section decrease in bedding dip, from subvertical beds in lowermost strata (left) to subhorizontal strata at the top. The trace of the thrust is ~200 m to the left of photograph. Peaks visible in far background are Triassic carbonates in thrust-sheet hanging wall. (C) Line drawing from a photograph of mudstone-dominated growth strata that onlap the flank of a small-scale anticline (shown in Fig. 6C) within the western Nangqian basin, section D (Figs. 2 and 4). Note up-section decrease in bedding dip and thinning of beds toward fold. Total syndepositional rotation is 10°–20°. (D) Line drawing from a photograph of onlap relationship between basin fill and flank of a basin-margin anticline, western Nangqian basin, basal section D (Figs. 2 and 4). Note the dominance of relatively fine grained deposits, particularly for strata along the structural margin of a basin.

The presence of growth strata in upper stratigraphic levels along the southwest margin (sections A and D in Figs. 2, 4, and 5, C and D) and northeast margin (sections G and L in Figs. 2 and 4) of the Nangqian basin indicates that the northeast-directed Jiangda thrust and southwest-directed Nangqian thrust were active during the latter stages of Paleocene–Eocene basin development. Similarly, the presence of growth strata in the Shanglaxiu basin (sections U–Y in Figs. 2, 4, and 5, A and B) indicates syndepositional motion along the northeast-directed Shanglaxiu thrust. Syncontractional sedimentation in the Niuguoda basin is confirmed by growth strata in the footwall of the southwest-directed Niuguoda thrust (section P in Figs. 2 and 4). An absence of growth-strata relationships in the Xialaxiu ba-

sin (sections Q–T in Figs. 2 and 4) may reflect erosional removal of proximal, basin-margin growth strata. Because fold-thrust structures were actively forming during Paleocene–Eocene basin development in the Nangqian-Yushu region, we consider the activation of sediment source areas and basin subsidence to be direct results of contraction (e.g., Talling et al., 1995; Horton, 1998; Lawton et al., 1999).

SEDIMENTARY FRAMEWORK

Depositional Environments

Basin fill studied in the 25 measured sections (Fig. 4) can be divided into facies associations representative of offshore lacustrine, nearshore

lacustrine, lacustrine fan-delta, and alluvial-fan environments. Table 1 provides complete descriptions of mudstone (M1, M2), sandstone (S1), conglomerate (G1, G2), carbonate (C1), and evaporite (E1) facies associations. Because facies descriptions are presented in Table 1, the following text focuses only on interpretations of depositional processes and environments.

Facies M1

Thick intervals (up to 500 m) of organic-rich mudstone deposits (Fig. 6A; Table 1), restricted to Cretaceous strata of the Nangqian basin, are attributed to suspension fallout in offshore lacustrine depositional environments (Link and Osborne, 1978). Rhythmic bedding indicates regular temporal variations in depo-

TABLE 1. SUMMARY OF FACIES ASSOCIATIONS

Facies	Description	Stratigraphic occurrence	Interpretation
M1	Thick intervals (up to 500 m) of gray mudstone and claystone with very thin siltstone interbeds (Fig. 6A). Organic matter is abundant and includes woody and cuticular matter. Palynomorphs and ostracods are present. Beds are 0.1–2.0 cm thick and generally calcareous. Colors include medium to dark gray, medium to dark green, violet, and yellow. Rhythmic bedding of millimeter- and centimeter-scale is defined by alternating intervals of variable color and induration.	Exclusively in Cretaceous strata of the lowermost fill in the southern part of Nangqian basin study area. Originally mapped as Jurassic (Qinghai BGMR, 1983a).	Offshore lacustrine environment. Preservation of organic matter may indicate generally humid climate.
M2	Poorly indurated, brick-red and buff-colored mudstone with thin interbeds of siltstone, minor claystone, and very fine grained sandstone. Individual mudstone beds are 0.1–5.0 cm thick and massive to poorly laminated (ripple cross-lamination and horizontal lamination) (Fig. 6D) with rare mudcracks. Generally occurs in continuous slope-forming intervals hundreds of meters thick (Fig. 6, B and C). Interbedded with facies S1, C1, E1, and G1.	Dominant in middle to upper Nangqian basin and prevalent throughout Xialaxiu and northern Shanglaxiu basins. Volumetrically, M2 and S1 compose the largest component of basin fill in the region.	Offshore lacustrine environment. General lack of desiccation features and pedogenic structures suggests minimal subaerial exposure and no soil development.
S1	Thin- to medium-bedded, fine- to medium-grained sandstone. Beds are 1–25 cm thick, have nonerosional basal contacts, and are moderately well sorted with poorly developed normal grading (Fig. 7, A–C). Sedimentary structures include horizontal and ripple cross-stratification, primary current lineations, and limited trough cross-stratification, bioturbation, burrows, and root traces. Fluid-escape structures and intrastratal contortions are common. Generally interbedded with facies M2, G1, G2, and C1.	Present mainly in middle Nangqian basin and throughout Niuguoda, Xialaxiu, and Shanglaxiu basins. S1 and M2 compose the largest volume of basin fill in the region.	Medial to distal fan delta. Fluid-escape structures indicate rapid depositional events.
C1	Medium- to thick-bedded, light gray carbonate (Fig. 7D). Primarily micrite with poor horizontal laminations. Recrystallized sparite and calcite veins are common. Fossil mollusks have been reported by Qinghai BGMR (1983a, 1983b). Beds are 0.5–5.0 m thick. Occurs interbedded with facies M2, S1, G1, and G2 or, less commonly, as continuous, stacked carbonate beds.	Exclusively in upper levels of Nangqian, Niuguoda, and Xialaxiu basins.	Carbonate precipitation in nearshore lacustrine environment.
E1	Thin- to medium-bedded, massive to poorly laminated white gypsum. Beds are 0.1–0.5 m thick. Exclusively interbedded with facies M2.	Present only in upper Nangqian basin.	Evaporative (playa) lake.
G1	Medium-bedded, well-organized, light gray to red, sandy pebble-cobble conglomerate (Fig. 8, A–E). Beds are consistently 0.2–1.0 m thick and persist laterally for tens to hundreds of meters. Ungraded to normally graded. Poor subhorizontal stratification and very rare low-angle trough cross-stratification and clast imbrication. Clasts include Carboniferous–Triassic carbonate and sandstone. Interbedded with facies S1, M2, C1, and G2.	Major facies of Niuguoda, northern Xialaxiu, and Shanglaxiu basins; minor facies of Nangqian basin.	Hyperconcentrated flows, fluid-rich debris flows, and possible gravelly turbidity currents of both subaerial and subaqueous parts of a fan delta.
G2	Medium- to thick-bedded, moderately organized, light gray to red, cobble-boulder conglomerate (Fig. 8F). Beds are 0.5–5.0 m thick and laterally continuous for a few tens of meters. Ungraded to reverse graded. Erosional basal contacts with poor subhorizontal and trough cross-stratification and clast imbrication. Rounded clasts up to 2 m in diameter include Carboniferous–Triassic carbonate and sandstone. Interbedded with facies G1, S1, and C1.	Minor facies in upper levels of Nangqian, Niuguoda, Xialaxiu, and Shanglaxiu basins.	Poorly developed gravel bars in fluvial channels on alluvial fan.

sitional conditions (Ashley, 1975; Sturm and Matter, 1978). Preserved organic matter and dark outcrop colors suggest relatively humid conditions. A lack of such facies in younger strata throughout the region suggests that lake dynamics and possibly climatic conditions for Cretaceous deposition were distinct from Paleocene–Eocene conditions.

Facies M2

Similar to facies M1, massive to poorly laminated mudstone deposits of facies M2 (Fig. 6, B–D; Table 1) are interpreted as suspension-fall-out deposits in offshore lacustrine depositional environments (Link and Osborne, 1978). However, a lack of organic matter and fossils, a common brick-red color, and an association with minor evaporite facies suggest that deposition of facies M2 occurred in a more oxidizing, more arid environment than that which characterized facies M1 deposition. Nevertheless, well-developed desiccation features and pedogenic facies are not present, suggesting only limited subaerial exposure and soil development.

Facies S1

Beds of this facies and facies M2 mudstone collectively form the greatest volume of basin fill in the region. Stratified sandstone of facies S1 (Fig. 7, A–C; Table 1) is attributed to subaqueous deposition of turbidity currents on medial to distal parts of a fan delta (Weirich, 1986; Horton and Schmitt, 1996) and to less common subaerial deposition of hyperconcentrated flows and fluid-rich debris flows on subaerial parts of a fan delta or alluvial fan (Smith, 1986; Blair and McPherson, 1994). Beds containing fluid-escape structures and intrastratal contortions suggest rapid depositional events on a saturated substrate (Postma, 1983), probably the submerged part of a fan delta. Deposits of more proximal fan environ-

ments are represented by interbedded conglomerate.

Facies C1

Massive carbonate beds of facies C1 (Fig. 7D; Table 1) are interpreted as deposits precipitated from solution in shallow waters of nearshore lacustrine environments (Kelts and Hsü, 1978). This facies is limited to the upper levels of the basins, suggesting conditions favorable for carbonate precipitation only during the latter stages of basin development. Because Carboniferous–Triassic carbonate rocks were exposed in sediment source areas throughout basin development, carbonate precipitation may record appropriate climatic conditions rather than bedrock-controlled water chemistry.

Facies E1

Thin-bedded evaporitic gypsum of facies E1 (Table 1) is attributed to precipitation in a playa-lake setting or along the evaporative margins of a lake (Hardie et al., 1978; Surdam and Stanley, 1979). This facies is rare and is restricted to the upper part of Nangqian basin fill. Therefore, the physical and chemical conditions governing carbonate sedimentation were also favorable for minor evaporite production.

Facies G1

Sandy pebble-cobble conglomerate of facies G1 is the most common coarse-grained facies in the region (Fig. 8, A–E; Table 1). These deposits are representative of sediment gravity flows, including sheet floods, hyperconcentrated flows, fluid-rich debris flows, and possible gravelly turbidity currents on both subaerial and subaqueous parts of a fan delta (Nemec and Steel, 1988; Blair and McPherson, 1994; Horton and Schmitt, 1996). Poorly developed sedimentary structures and a lack of channel geometries indicate limited development of bedforms or bars. Therefore, most deposition occurred during individual sedimentation events, as opposed to continuous filling of fluvial channels by well-developed bedforms or bar elements.

Facies G2

This rare coarse-grained facies consists of cobble-boulder conglomerate (Fig. 8F; Table 1) and is attributed to deposition of poorly developed gravel bars in channels on a proximal alluvial fan or subaerial part of a fan delta (Nemec and Postma, 1993; Ridgway and DeCelles, 1993). Despite large clast sizes, preserved sedimentary structures indicate deposition by erosive, turbulent water flows of high competence rather than by laminar debris flows. A lack of substantial debris-flow deposits throughout the basins may be attributable to a lack of fine-grained matrix in the carbonate-dominated source areas.

Facies Distribution

Both fine- and coarse-grained strata compose basin fill of the Nangqian-Yushu region. Coarse-grained fan deposits are generally confined to <5 km from basin margins; fine-grained lacustrine deposits occupy both the central axes and margins of basins (Fig. 2). Although inspection of measured sections (Fig. 4) suggests subequal amounts of fine- and coarse-grained strata, representations of their distribution in map view and cross section (Fig. 2) indicate that fine-grained strata are the most volumetrically significant deposits filling the basins (Fig. 9). This relationship is particularly striking because growth-strata relationships demonstrate that sedimentation was largely contemporaneous with fold-thrust deformation (Fig. 5). Therefore, both fine- and coarse-grained deposits record syncontractional sedimentation, underscoring the point that sediment grain size may not be a diagnostic indicator of tectonism (e.g., Heller et al., 1988; DeCelles et al., 1991).

Shifting of facies belts during basin development is evidenced by fining- and coarsening-upward patterns (Figs. 3 and 4). In the Nangqian basin, lower stratigraphic levels are characterized by localized conglomeratic units in the southern and northern parts of the basin (sections A, B, and K in Fig. 4). In contrast, upper levels of the basin are dominated by fine-grained lacustrine deposits that can be traced laterally across most of the basin (sections C–M in Fig. 4). Therefore, the Nangqian basin initially developed as several isolated fan depocenters but evolved into a single broad lacustrine basin by latter stages of basin filling. All basins show a similar up-section trend toward more lacustrine, particularly carbonate, facies (Figs. 3 and 4).

Although structural overlap by thrust faults may obscure a few kilometers of the most proximal basin fill, preservation of proximal facies and growth strata along basin margins suggests that the present-day outcrop belts approximate the original dimensions of the basins (Fig. 9). Therefore, the basins evolved as distinct entities separated by fold-thrust structures rather than as a large contiguous basin that was broken into several outcrop belts by later deformation.
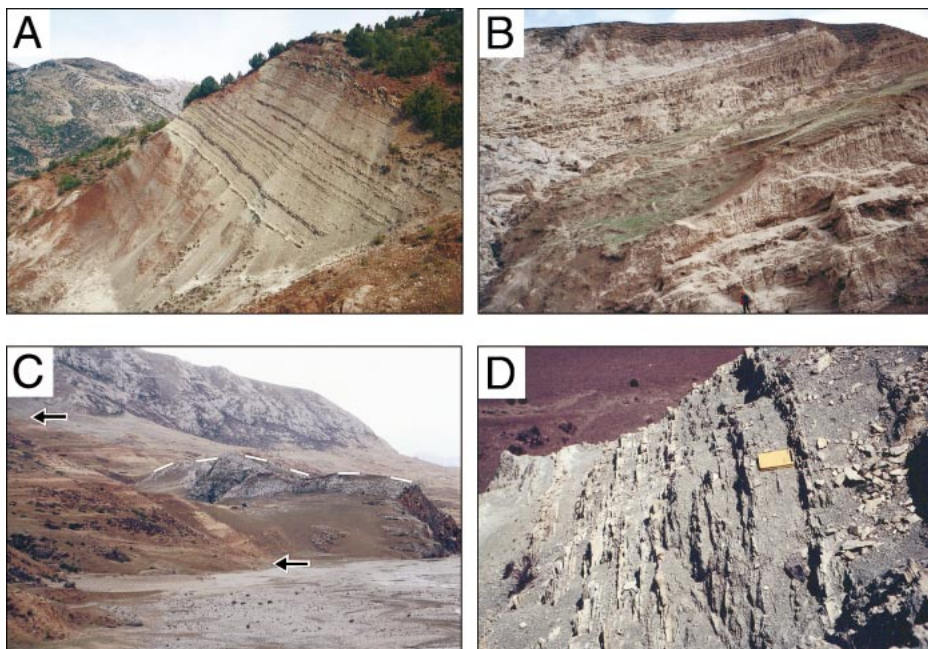
Provenance

Paleocurrent data and conglomerate compositional analyses provide information on the location and composition of numerous sediment source areas during basin development. Over 1500 paleocurrent measurements are predominantly from the limbs of medium-scale trough cross-stratification developed in sandstone and conglomerate (Fig. 4). Additional measurements include primary current lineations, ripple marks, sole marks, and clast imbrications. Compositional data are from >150 clast counts (~100 clasts identified per count), each performed over an ~1 m^2 area on individual conglomerate outcrops (Fig. 4). Table 2 summarizes the paleocurrent and clast compositional data from the measured sections and our interpretations of the associated sediment source areas, structural features, and depositional systems. The interpretations in Table 2 are best understood by joint inspection of the structural cross section (Fig. 2B) and provenance data (Fig. 4).

Clast-count data indicate that conglomerates were almost exclusively derived from three Carboniferous units and four Triassic units composed of carbonate, quartz sandstone, quartzite, and argillite (Table 2). A few rare volcanic clasts present in the Xialaxiu basin (base of section T in Fig. 4) were probably derived from limited Triassic volcanic beds. The only igneous clasts derived from Tertiary intrusions or volcanic units occur in the uppermost levels of the Nangqian basin (section F in Fig. 4). In some cases, unique varieties of clasts can be directly linked to nearby source areas. For instance, on the basis of lithologies found in Carboniferous–Triassic exposures, the only possible source area of rare olive-green argillite clasts found in fill of the western Nangqian basin (section C in Fig. 4) is the argillite-bearing Carboniferous rocks (unit C1) along the western margin of that basin (Fig. 2). The relatively limited number of Carboniferous–Triassic source units and the lack of pre-Carboniferous detritus may suggest fairly limited erosional unroofing during basin development.

In most cases, paleocurrent data and lateral variations in grain size implicate the nearest basin-margin structure as the primary sediment source (Figs. 4 and 9). For example, mainly north-directed paleocurrents and northward fining within the Shanglaxiu basin (intermediate levels of sections V–X in Fig. 4) suggest sediment derivation from the Shanglaxiu thrust sheet to the south. Paleocurrents are predominantly directed toward basin centers, supporting facies relationships (as already described) indicating no

Figure 6. Representative photographs of mudstone facies associations. (A) A 50-m-thick section of mudstone and claystone (facies M1) of variable color and induration. Section B, 100–150 m level, Cretaceous strata, Nangqian basin. (B) View of 150-m-thick interval of mudstone (facies M2) and minor interbedded sandstone. Person at base of photograph for scale. Section T, 440–590 m level, northern Xialaxiu basin. (C) View of 180-m-thick section of subhorizontal siltstone (facies M2) and minor fine-grained sandstone overlapping the crest of an intrabasinal anticline (denoted by white line segments). Arrows denote bottom and top of section. Ridgeline forming the skyline is composed of Carboniferous carbonate. Section D, western Nangqian basin. (D) A 3.5-m-thick interval of thin-bedded, calcareous claystone and mudstone (facies M2). Notebook (20 cm) for scale. Section F, 550 m level, central Nangqian basin.

connection among the drainage systems of the different basins (Fig. 9).

BASIN DEVELOPMENT

Temporal changes in sedimentology, stratigraphy, and provenance provide an account of the varying sedimentation history (Table 2; Fig. 4), which in turn serves as the foundation for a reconstruction of basin 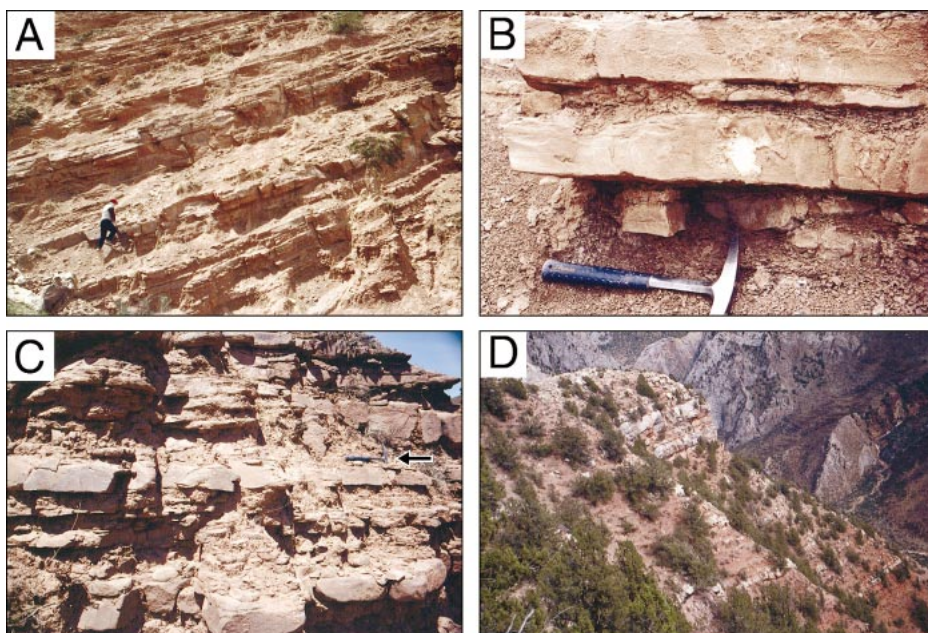development and associated deformation in the Nangqian-Yu-shu region (Fig. 10). In this reconstruction, proposed phases of deformation along specific structures are based on measured paleocurrent patterns, compositional trends, depositional systems, and growth-strata geometries.

Mesozoic Denudation and Initial Sedimentation in the Nangqian Basin

In the Nangqian basin, a possible phase of Mesozoic denudation is expressed by the unconformity between Cretaceous–Paleogene deposits above and Carboniferous rocks below (Fig. 2). The absence of Triassic rocks, which are pervasive north of the Nangqian fault zone (Fig. 2), suggests either nondeposition or erosional denudation of Triassic rocks in the Nangqian basin area. Mesozoic erosion in this part of the Qiangtang terrane may be attributable to deformation related to latest Triassic collision with the Songpan-Ganzi terrane (e.g., Dewey et al., 1988; Kapp et al., 2000), Late

Figure 7. Representative photographs of sandstone and carbonate facies associations. (A) A 15-m-thick interval of thin-bedded sandstone (facies S1) and minor mudstone. Person at left for scale. Section K, ~1000 m level, northern Nangqian basin. (B) Two normally graded sandstone beds (facies S1) and overlying siltstones. Each sandstone exhibits a massive to horizontally stratified base, ripple cross-stratified top, and overlying laminated siltstone. These units are interpreted as nearly complete Bouma sequences. Hammer (30 cm) for scale. Section R, ~330 m level, southern Xialaxiu basin. (C) A 3-m-thick interval of thin- to medium-bedded sandstone (facies S1). Sandstone beds exhibit plane-parallel lamination, ripple cross-lamination, minor bioturbation, and rare root traces. Hammer (30 cm) at right-center (arrow) for scale. Section K, 625 m level, northern Nangqian basin. (D) View of 150-m-thick section composed of thick-bedded carbonate ledges (facies C1) and slope-forming siltstone and fine-grained sandstone. Section G, 65–215 m level, Nangqian basin.
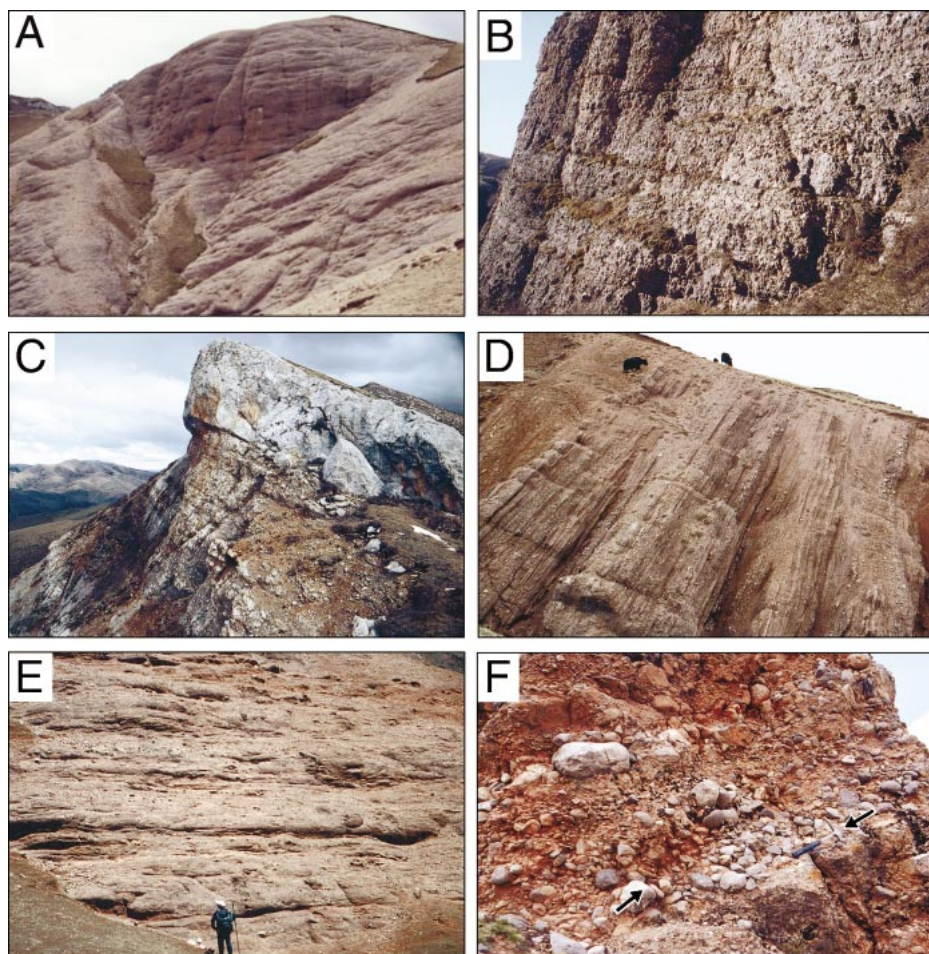
Figure 8. Representative photographs of conglomerate facies associations. (A) Smooth face of 140-m-thick outcrop of well-organized, horizontally stratified, cobble conglomerate (facies G1). Section T, 1190–1330 m level, northern Xialaxiu basin. (B) A 30-m-thick exposure of moderately organized, well-bedded, cobble conglomerate (facies G1). Section W, 0–30 m level, Shanglaxiu basin. (C) An ~120-m-thick section composed of cobble conglomerate (facies G1) capped by a 25-m-thick carbonate ledge. Section T, 1635–1755 m level, northern Xialaxiu basin. (D) A 50-m-thick interval of well-organized, sandy pebble-cobble conglomerate (facies G1), interbedded sandstone, and capping siltstone. Yak (~1 m tall) for scale. Section S, 800–850 m level, southern Xialaxiu basin. (E) An 11-m-thick interval of even-bedded, sandy pebble-cobble conglomerate (facies G1) and interbedded sandstone. Slightly contorted bedding contacts are the product of syndepositional loading. Sandstones contain abundant fluid-escape structures. Person for scale. Section P, 350 m level, northern Niuguoda basin. (F) A 3.5-m-thick outcrop of poorly organized, well-rounded cobble-boulder conglomerate (facies G2) exhibiting horizontal stratification, trough cross-stratification, and clast imbrication. Hammer (30 cm) parallels bedding (right arrow). Left arrow is parallel to inclined, subplanar foreset of trough-cross bed. Section O, 40 m level, central Niuguoda basin.

Jurassic–Early Cretaceous collision with the Lhasa terrane (e.g., Allègre et al., 1984; Burg and Chen, 1984; Murphy et al., 1997; Yin and Harrison, 2000), or intracontinental Jurassic–Early Cretaceous extension that is widespread in northern Tibet (Huo and Tan, 1995).

Initial sediment accumulation during middle Cretaceous time involved lacustrine deposition of fine-grained, organic-rich strata in the southern Nangqian basin study area (lower parts of sections A and B in Fig. 4). Although the base of the section is not exposed, this mudstone interval is potentially underlain by Jurassic rocks that have been mapped for several hundred kilometers to the south-southeast (Liu, 1988; Qinghai BGMR, 1991). The Ju-

rassic and Cretaceous fine-grained sedimentary rocks may have had an origin similar to that of widespread Jurassic–Cretaceous deposits over much of southeastern Tibet and Yunnan province, south China (Huang et al., 1992). Without further regional analyses, interpretations of both the Mesozoic phase of denudation and the origin of mid-Cretaceous sedimentation remain speculative.

Initial Paleocene–Eocene Syncontractional Basin Development

Early Tertiary syncontractional sedimentation was related to motion along several basin-bounding thrusts (Fig. 10A; Table 2). In the southern Nangqian basin, fine-grained Cretaceous deposits are overlain by a thick section of dominantly fan-delta conglomerate (sections A and B in Fig. 4). The coarse-grained fill was derived from the northeast (section A) and southwest (section B), suggesting initial motion on the southern traces of the Nangqian and Jiangda thrusts at this time. A thick conglomerate section was also deposited locally in the northern Nangqian basin (lower part of section K in Fig. 4). This conglomerate was derived from the northeast during inferred southwest-directed thrusting along the northern trace of the Nangqian thrust system (Fig. 10A; Table 2).

Early sedimentation in basins north of the Nangqian basin is correlated with initial Nangqian conglomerate deposition. The Niuguoda basin was filled by sandstone and conglomerate derived from the northeastern margin of the basin (section P in Fig. 4), presumably during motion on the Niuguoda thrust (Fig. 10A).

The Xialaxiu basin was initially supplied by both fine- and coarse-grained sediment (sections R–T in Fig. 4) from a northwestern source (Fig. 10A). This roughly axial sedimentation may have been related to fold-thrust deformation near basin margins.

The Shanglaxiu basin developed during shortening along the northern and southern margins of basins (Fig. 10A). The northeastern margin served as a continuous source of sandstone and conglomerate, possibly derived from the trailing limb of a hanging-wall anticline (sections U–X in Fig. 4). The Shanglaxiu thrust along the southwestern margin was active during basin sedimentation, as demonstrated by growth strata in the footwall of the thrust (sections U–Y in Figs. 2, 4, and 5, A and B). A general fining of deposits from south to north (sections V–Y in Fig. 4) further indicates that the Shanglaxiu thrust was the principal sediment source for the basin.
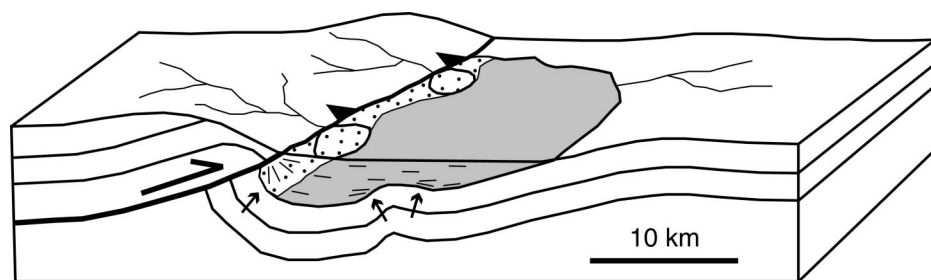
Figure 9. Schematic block diagram of basin development in the Nangqian-Yushu region. Basin subsidence occurs in footwall of active thrust fault. Small drainage networks provide sediment derived from Carboniferous–Triassic rocks (no pattern). The basin is dominated volumetrically by fine-grained lacustrine deposits (shaded); proximal conglomeratic facies (random-dot pattern) are confined to the faulted margin of the basins. Most sediment is derived from thrust-sheet hanging wall. Bedding orientations (short line segments) show growth-strata geometries adjacent to thrust and on flanks of small anticline (small arrows).

Late-Stage Paleocene–Eocene Syncontractional Basin Development

Further basin development during the early Tertiary involved continued and newly activated motion on several thrust faults (Fig. 10B; Table 2). Whereas dominantly fine-grained lacustrine strata were deposited over most of the elongate Nangqian basin (sections C–M in Figs. 2 and 4), localized coarse-grained sedimentation suggests relative uplift along basin flanks (Fig. 10B). Growth-strata relationships along the northern trace of the Jiangda thrust (section D in Figs. 2 and 4) indicate syndepositional deformation on the floor of a lake (Fig. 5C) and along the northwestern margin of basin (Fig. 5D). Local coarse-grained deposits along the northeastern flank of the basin (sections F, G, H, I, L, and M in Fig. 4) overlie, and are cut by, southwest-directed imbricate thrust splays linked to the Nangqian fault zone (Fig. 10B).

The Niuguoda basin was characterized by the inception of a southwest-directed imbricate thrust fault linked to the Niuguoda thrust (Fig. 10B). Growth strata are locally present in the footwall of the imbricate thrust, indicating deposition of fan-delta conglomerate and lacustrine carbonate (section P in Figs. 2 and 4) coeval with deformation along the northeastern margin of the basin.

Activation of the Xialaxiu thrust along the southwestern margin of the Xialaxiu basin occurred late in the basin's depositional history (Fig. 10B). Late-stage sedimentation in the basin included accumulation of lacustrine carbonates and conglomerates in an alluvial fan or fan delta derived from the hanging wall of the Xialaxiu thrust (sections Q–T in Fig. 4). Little sediment is derived from northern areas, suggesting cessation of motion on structures to the north.

Final accumulation in the Shanglaxiu basin involved deposition of an east-derived conglomerate unit (sections U and V in Fig. 4). This conglomerate unconformably overlaps the Shanglaxiu thrust, indicating that the fault was inactive by this time (Fig. 10B).

Magmatism and Strike-Slip Faulting Following Basin Development

Igneous rocks and right-lateral faulting postdate most of the basin development (Fig. 10C; Table 2). To the north, intrusions and volcanic rocks in the Shanglaxiu basin have been dated at 51.2 ± 0.2 Ma to 49.5 ± 0.2 Ma (Spurlin et al., 2000). The intrusions cut the lower part of the basin, and the volcanic rocks unconformably overlie the basin (Fig. 2), thus providing a minimum age for the Shanglaxiu basin. To the south, the Nangqian basin was the site of significant volcanism and related intrusion in late middle Eocene time. Ages for volcanic and intrusive rocks range from 38.2 ± 0.1 Ma to 37.0 ± 0.2 Ma (Spurlin et al., 2000). The volcanic rocks are interbedded with uppermost basin fill of the northernmost Nangqian basin (e.g., sections E, F, H, I, and K in Fig. 4). On the basis of along-strike correlations, the volcanic strata entirely postdate fill in areas of the Nangqian basin to the south. Intrusions are also limited to the northernmost Nangqian basin and cut the intermediate to upper levels of the succession (sections J–L in Fig. 4). This age constraint indicates that syncontractional

sedimentation was complete by approximately 37 Ma.

Initiation of right-lateral strike-slip faults postdated basin development (Spurlin et al., 2000). Several right-slip faults cut uppermost strata of the Nangqian basin, including upper middle Eocene (38–37 Ma) igneous rocks that mostly postdate basin development. The temporal and kinematic relationship between the right-slip faults we mapped in the Nangqian area and the relatively recent (Quaternary and possibly earlier) left-slip Ganzi-Yushu fault (Wang and Burchfiel, 2000), which bounds the northern limit of the study area ~70 km to the north (Fig. 2), is unknown.

Basin Summary

Sedimentary, structural, and provenance relationships indicate that the basins of the Nangqian-Yushu region developed as disconnected basins during syndepositional Paleocene–Eocene contraction. The timing of this deformation, which involved >50 km of northeast-southwest shortening, is defined by age data from fossil assemblages, interbedded tuffs, overlapping volcanic rocks, and cross-cutting intrusions. Although one basin (the Nangqian basin) has a history of mid-Cretaceous sedimentation, the lack of a direct link with contractional deformation makes the structural setting of this early sedimentation unclear. Although we cannot rule out possible Cretaceous shortening in the region, the Paleogene fossils, lower to middle Eocene igneous rocks, and growth-strata relationships in upper stratigraphic levels collectively suggest a principally Paleocene through middle Eocene age of sedimentation and associated shortening in the Nangqian-Yushu region. Following basin development, strike-slip deformation produced >15 km of cumulative right-lateral offset in the region.

DISCUSSION

Sedimentologic, stratigraphic, compositional, and structural data from the basins of the Nangqian-Yushu region enable us to address several problems concerning the tectonic and geomorphic evolution of the east-central Tibetan plateau. First, our analysis provides initial constraints on the timing, magnitude, and style of deformation in the Nangqian-Yushu region of east-central Tibet. We find that crustal shortening expressed by thin-skinned thrusting occurred in this region during the very early (Paleocene–Eocene) stage of the India-Asia collision. Second, although large modern river systems are eroding part of east-

TABLE 2. SUMMARY OF PROVENANCE, STRUCTURES, AND DEPOSITIONAL SYSTEMS RELATED TO BASIN DEVELOPMENT

Measured section	Conglomerate clast composition and up-section variation	Paleoflow direction	Interpretation of sediment source area, related structural features, and basin depositional systems
Nangqian basin, west and southwest margin			
B	Carbonate dominant throughout conglomeratic section.	northeast-directed	Prolonged erosion of Carboniferous carbonate (C2) in hanging wall of northeast-directed Jiangda thrust fault along southwestern margin of basin. Transverse drainage and alluvial-fan deposition.
C–E	Carbonate dominant at base, increased argillite and limited sandstone up section.	east-directed	Erosion of Jiangda fold-thrust structure along western margin of basin: initial erosion of Carboniferous carbonate (C2) with increased input from Carboniferous clastic units (C3) through time. Transverse drainage and deposition in fan-delta and offshore lacustrine environments.
A	Carbonate dominant at base of conglomeratic section, increased sandstone followed by increased carbonate up section, presence of argillite only at 1100–1300 m level.	west-directed	Prolonged erosion of Triassic carbonate (Tr2) and Triassic or Carboniferous clastic units (Tr3 or C3) along eastern margin of basin: erosion of hanging wall of southwest-directed Nangqian thrust system (Tr2, Tr3) and possible erosion of C3 in fold-thrust structures in footwall (now covered by younger basin fill). Increase in carbonate (Tr2) at higher stratigraphic levels may reflect final phase of reverse slip on the Nangqian thrust system. Transverse drainage and deposition in fan-delta environment.
Nangqian basin, east and northeast margin			
G–M	Carbonate dominant at base, increased sandstone followed by increased carbonate up section.	mostly west-directed	Prolonged erosion of Triassic carbonate (Tr2) along northeastern margin of basin in hanging wall of southwest-directed Nangqian thrust system followed by initial erosion of Carboniferous sandstone (C1) in footwall. Increase in carbonate at higher stratigraphic levels may reflect final phase of reverse slip on the Nangqian thrust system. Mostly transverse drainage and deposition in alluvial-fan, fan-delta, and nearshore lacustrine environments.
F	Volcanic rocks and limited sandstone.	?	Erosion of Eocene volcanic rocks and Carboniferous sandstone (C1) in footwall of Nangqian thrust system. Unknown drainage, volcanic and sedimentary deposition in nearshore and offshore lacustrine environments.
Niuguoda basin			
P	Mixed carbonate and sandstone at base and generally increased carbonate up section with fluctuations in amount of sandstone and chert.	southwest-directed	Prolonged erosion of Triassic carbonate (Tr2) and sandstone (Tr3) in hanging wall of southwest-directed Niuguoda thrust along northeastern margin of basin. Increase in carbonate at higher stratigraphic levels may reflect erosional stripping of most Triassic sandstone (Tr3). Transverse drainage and deposition in fan-delta, alluvial-fan, and fluvial environments.
N, O	Carbonate dominant, very limited sandstone.	southwest- and south-directed	Erosion of Triassic carbonate (Tr2) and limited sandstone (Tr3) along northeastern margin of basin: combined erosion of hanging wall of southwest-directed Niuguoda thrust and its footwall imbricate thrust. Deposition in transverse alluvial fan and possible axial fluvial system.
Xialaxiu basin, southwest margin			
Q–S	Carbonate dominant at base, increased sandstone followed by increased carbonate up section.	base: south-directed; top: mostly northeast-directed	Initial erosion of Triassic carbonate (Tr4) along northern margin of basin followed by erosion of Triassic sandstone (either Tr3 along northern margin of basin and/or Tr1 in hanging wall of southwest-directed thrust farther north). Late-stage erosion related to northeast-directed Xialaxiu thrust system along southwestern margin of basin provided Triassic carbonate (Tr2) during final clastic sedimentation in the basin. Variable drainage, deposition in fan-delta and nearshore and offshore lacustrine environments.
Xialaxiu basin, northeast margin			
T	Volcanic dominant in lower levels, mixed argillite, carbonate, and sandstone in middle levels, carbonate and limited sandstone in upper levels, monolithologic carbonate at top.	lower: southeast-directed; top: north-directed	Initial erosion of Triassic volcanic rocks (Tr1?) to north and west of basin. Prolonged erosion of mostly Triassic carbonate (Tr4, Tr2?) and limited Triassic sandstone and argillite (Tr3, Tr1?) within folds along northern margin of basin and hanging wall of southwest-directed thrust farther north. Late-stage erosion of Triassic carbonate (Tr2) along southern margin of basin yielded monolithologic gravel synchronously with lacustrine carbonate deposition in the basin. Mostly axial drainage, deposition in fan-delta, alluvial-fan, and nearshore and offshore lacustrine environments.
Shanglaxiu basin, south margin			
U	Carbonate dominant at base, increased sandstone followed by increased carbonate up section.	base: south-directed; top: west-directed	Late-stage erosion of Triassic carbonate (Tr4, Tr2?) and limited Triassic sandstone (Tr3, Tr1?) from anticline east-northeast of basin. Deposition postdates final motion of northeast-directed Shanglaxiu basin, south margin. Axial and transverse drainage, alluvial-fan and fluvial deposition.
Shanglaxiu basin, central			
V–X	Carbonate dominant at base, minor increased sandstone followed by increased carbonate up section.	base: northwest-directed; top: mostly north-directed	Prolonged erosion of Triassic carbonate (Tr4, Tr2?) and limited Triassic sandstone (Tr3, Tr1?) from anticline east-northeast of basin and erosion of mostly Triassic carbonate (Tr2) in hanging wall of northeast-directed Shanglaxiu thrust (southern segment). Base: transverse drainage and alluvial-fan deposition. Top: axial drainage and deposition in alluvial-fan, fan-delta, and nearshore lacustrine environments.
Shanglaxiu basin, north margin			
Y	Carbonate dominant throughout.	northeast-directed	Late-stage erosion of Triassic carbonate (Tr2) in hanging wall of northeast-directed Shanglaxiu thrust (north segment). Transverse drainage and alluvial-fan or fan-delta deposition.

Note: Lithologic units correspond to map units (Carboniferous: C1, C2, C3; Triassic: Tr1, Tr2, Tr3, Tr4) shown in Figure 2, based on Qinghai BGMR (1983a, 1983b) and Spurlin et al. (2000). Question marks convey uncertainty on particular sediment source units.

ern and southern Tibet (Fig. 1; Yellow, Yangtze, Mekong, Salween, and Tsangpo Rivers; Brookfield, 1998; Métivier et al., 1999; Hallet and Molnar, 2001; Zeitler et al., 2001), the initiation ages of these rivers are not well established. For the Nangqian-Yushu region, sedimentologic and compositional analyses of basin fill help us define depositional systems, estimate the size of erosional drainage networks and associated rivers, and evaluate the degree of denudation in adjacent deforming source areas.
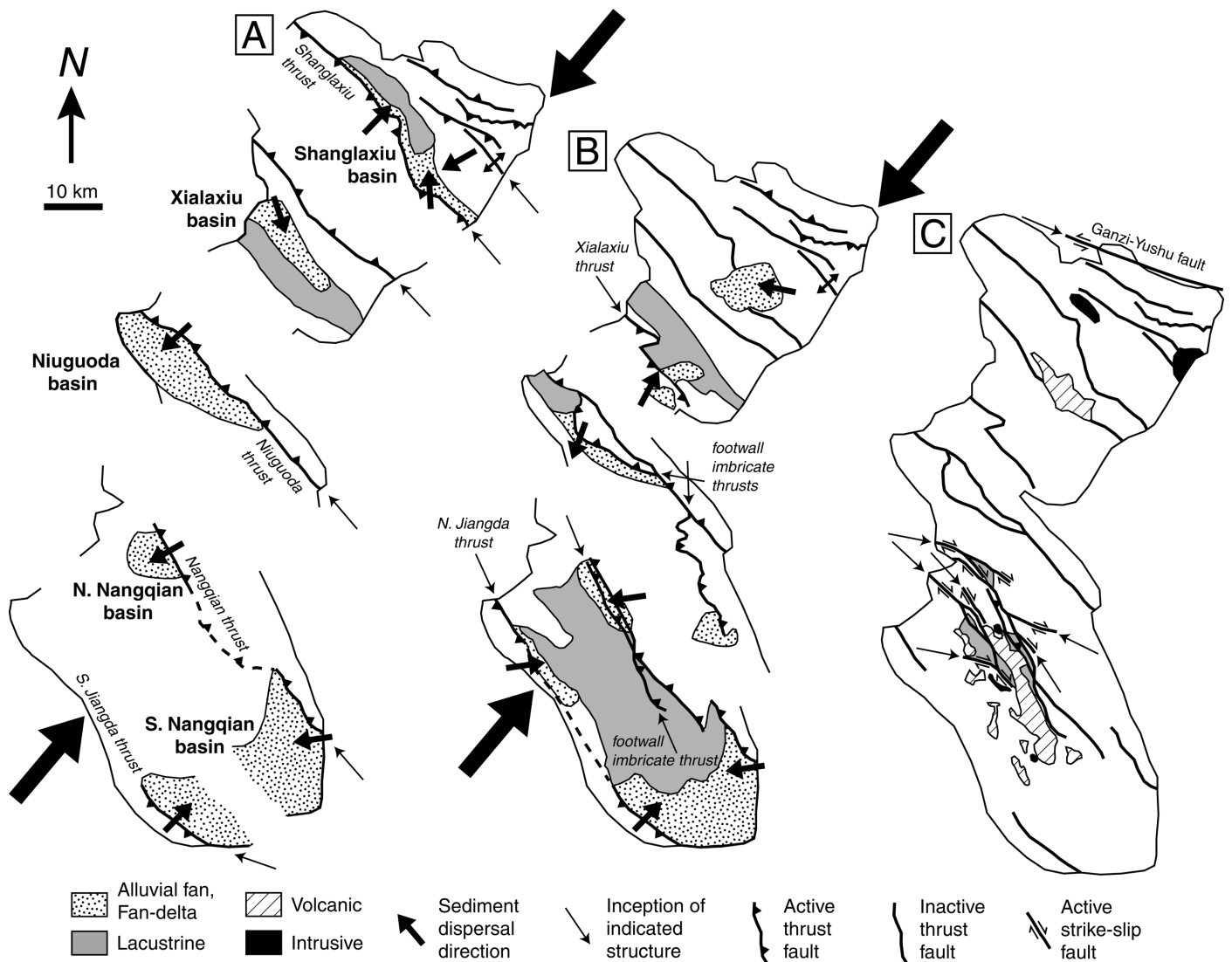
Figure 10. Three-phase reconstruction of basin development and related deformation in Nangqian-Yushu region (based on data and interpretations presented in Fig. 4 and Table 2). Irregular outline corresponds to mapped area in Figure 2. Palinspastic restoration includes ~50 km of northeast-southwest shortening (denoted by large arrows). (A) Initial Paleocene–Eocene basin development synchronous with northeast- and southwest-directed thrusting. (B) Late-stage Paleocene–Eocene basin development during final shortening, including motion on existing and newly activated northeast- and southwest-directed thrusts. (C) Final sedimentation in the Nangqian basin is mostly postdated by 38–37 Ma magmatism and subsequent right-lateral strike-slip deformation.

Crustal Shortening and Syncontractional Sedimentation

Deformation synchronous with Paleocene–Eocene basin development in the Nangqian-Yushu region was expressed by northeast- and southwest-directed thrusting. The timing of this shortening is provided by Paleogene fossils within syncontractional strata, lower Eocene (51–49 Ma) igneous rocks postdating the syncontractional Shanglaxiu basin, and upper middle Eocene (38–37 Ma) volcanic rocks interbedded with strata of the uppermost Nangqian basin. This record of early Tertiary deformation provides evidence for shortening in east-central Tibet coeval with the initial stage of the India-Asia collision, which may have begun as early as approximately 70 Ma (see review by Yin and Harrison, 2000). This shortening, along with early Tertiary contraction in central Tibet along the Bangong-Nujiang suture zone (Kapp et al., 1999; Yin and Harrison, 2000), in north-central Tibet along the Jinsha suture zone (Leeder et al., 1988; Yin and Nie, 1996; Liu et al., 2001), and in the Tethyan Himalaya fold-thrust belt (Ratschbacher et al., 1994) south of the Indus-Yalu suture zone, probably accommodated several hundred kilometers of India-Asia convergence during the early phase of the collision. Continued convergence may have been similarly accommodated by Oligocene–Miocene contraction along the periphery of the Tibetan plateau, including continued shortening in the Himalayan fold-thrust belt (e.g., DeCelles et al., 1998), structural development of the Gangdese and Renbu-Zedong thrust systems in southern Tibet (Yin et al., 1994, 1999), and thrusting along the extreme northern margin of Tibet (e.g., Sobel and Dumitru, 1997; Meyer et al., 1998).

The final stages of basin development in the

Nangqian-Yushu region mostly preceded, but locally accompanied, the late middle Eocene (38–37 Ma) magmatism in the northern Nangqian basin (Fig. 10). Therefore, we suggest that sediment accumulation and fold-thrust deformation had terminated in the region by Oligocene time. Right-lateral strike-slip faulting postdated basin development (Fig. 10C). Although spatially coincident with some fold-thrust structures, this phase of faulting is distinguished from earlier shortening by a lack of basin development and a concentration of faulting in the northern Nangqian basin area. On the basis of the tectonic position of these faults, we suggest that the Nangqian right-slip faults represent the northern continuation of the Batang-Lijiang right-lateral strike-slip system (Ratschbacher et al., 1996; Wang et al., 2001). This Neogene right-slip system may have been active synchronously with the left-slip Xiangshuihe-Xiaojiang and Ganzi-Yushu systems to the north (Fig. 2). Together, these fault systems may have assisted southeastward extrusion (Peltzer and Tapponnier, 1988) or clockwise rotation of the easternmost Tibetan block west of the Xiangshuihe-Xiaojiang fault zone (Royden et al., 1997; Wang and Burchfiel, 2000).

Sedimentation contemporaneous with shortening in the Nangqian-Yushu region involved primarily fine-grained lacustrine deposition; alluvial-fan and fan-delta deposition was narrowly limited to basin margins (Figs. 9 and 10, A and B). Preserved proximal facies and growth strata along the margins of outcrop belts (Fig. 2) and a lack of single lithostratigraphic units that can be correlated regionally among the basins (Fig. 3) indicate that the basins developed as distinct, isolated features with dimensions approximately similar to their present-day outcrop areas (generally <10³ km²). The basins are narrow (<15 km wide), shallow (<2 km deep), elongate features parallel to bounding thrust faults.

In comparison to other sedimentary basins along strike to the northwest and southeast, the basins of the Nangqian-Yushu region are broadly similar in terms of age, geometry, depositional environments, and related structures. Lower Eocene through lower Miocene strata to the northwest in the Fenghuo Shan region (Leeder et al., 1988; Liu and Wang, 2001; Liu et al., 2001) and upper middle Eocene to Oligocene strata to the southeast in basins of southeastern Tibet and Yunnan province (Gongjue, Lijian, and Jinggu basins) (Meyerhoff et al., 1991; Wang, 1995; Wang et al., 2001) (Fig. 1) contain proportions of lacustrine, fan-delta, and alluvial-fan strata similar to the basins of the Nangqian-Yushu re-

gion. A possible predominance of fine-grained lacustrine detritus in the basins of the Tibetan plateau interior may indicate small, poorly integrated drainage systems across much of Tibet during early Tertiary time (see next section). Throughout the Fenghuo Shan to Yunnan region, locally derived nonmarine deposits probably represent syncontractional basin development (Leeder et al., 1988; Liu and Wang, 2001; Liu et al., 2001; Wang et al., 2001; this study). The basins throughout this belt are commonly elongate features exhibiting length:width ratios commonly greater than 10:1 (Fig. 1). We suggest that the narrow basin widths (generally <15 km and locally <5 km) in the Nangqian-Yushu region were controlled by the spacing of Paleocene–Eocene thrusts. As exemplified in our structural cross section (Fig. 2B), narrow thrust spacing may be the product of a relatively shallow (~5-km-deep) décollement from which individual thrusts cut up through the Carboniferous–Triassic section to create isolated syncontractional basins. The limited thickness of basin fill may be attributable to limited subsidence of the footwall due to local block tilting, similar to piggyback basins in thin-skinned fold-thrust belts (Ori and Friend, 1986; Talling et al., 1995). Alternatively, basin dimensions could reflect highly localized flexural responses to small-scale thrust loading on a weak (low flexural rigidity) crust. In either case, these plateau-interior basins are inherently different from the foredeep basins formed by regional flexural subsidence along the periphery of the Himalayan-Tibetan orogen, including the Qaidam (Bally et al., 1986; Song and Wang, 1993; Métivier et al., 1998), Tarim (Graham et al., 1993; Sobel and Dumitru, 1997), Sichuan (Chen et al., 1995) and Himalayan basins (Burbank et al., 1996; DeCelles et al., 1998).

Erosion and Geomorphic Conditions

The sedimentologic and compositional histories of the basins of the Nangqian-Yushu region indicate internal drainage and low erosional denudation, similar to modern geomorphic conditions across much of the interior of Tibet. Internal drainage for each of the basins is suggested by centrally directed paleocurrents, dominantly lacustrine depositional conditions, and the overall distribution of facies (coarse-grained facies limited to basin margins and a lack of regionally correlative strata) (Fig. 9). Given the lateral spacing of basins at 20 km or less, even when palinspastically restored (Fig. 10), it is improbable that individual drainage networks exceeded 10³ km² in area. The globally observed rela-

tionship between drainage area (A) and mainstem river length (L) in modern river systems ($L = 1.75A^{0.52}$) (Hack, 1957; Montgomery and Dietrich, 1992) suggests that individual rivers within the Nangqian-Yushu region were generally no more than 50 km long. Average sediment-accumulation rates calculated from new age data also allow an approximation of denudation rates. Deposition of a composite 2000-m-thick succession in the Nangqian basin from middle Cretaceous to late middle Eocene time yields a long-term, undecompacted, average sediment-accumulation rate of ~30 m/m.y. (0.03 mm/yr). Because most sediment accumulated continuously in lacustrine settings where accommodation space exceeds sediment supply (Einsele and Hinderer, 1998), this extremely low accumulation rate requires a low volume of sediment supplied by erosional denudation. In other words, because there is no significant volumetric loss of sediment in these dominantly lacustrine basins, the sediment-accumulation rates are a direct proxy for denudation in the source area. Limited denudation is consistent with provenance data that indicate erosion of only a few Carboniferous–Triassic source units, without exposure of older Paleozoic units.

Further evidence for limited denudation is provided by facies patterns and paleocurrent data (discussed previously) indicating that the basins developed in their approximate present-day outcrop extent (Fig. 9). Such preservation of basin fill suggests that there has not been substantial erosion of the region since the termination of basin development. Therefore, evolution of the headwaters of two major rivers that now cross this part of east-central Tibet, the Yangtze and Mekong Rivers, probably occurred during the Neogene, after basin development. Indeed, the predominance of lacustrine deposits—the sources of which were small drainage networks with short-length rivers, rather than large river systems or fluvial megafans derived from extensive drainage networks (e.g., Horton and DeCelles, 2001)—requires that large rivers were not present in the Nangqian-Yushu region during early Tertiary basin development. These findings are at odds with recent suggestions that major rivers of eastern Tibet were established by earliest Tertiary time (Brookfield, 1998; Hallet and Molnar, 2001). Instead, we propose that the deeply incised rivers in eastern Tibet were established during the Neogene, consistent with the predominantly Neogene increases in mass-accumulation rates documented at the mouths of major Asian rivers (Métivier et al., 1999). This proposal suggests that a limited amount of detritus escaped off the eastern margin of

the Tibetan plateau prior to the Neogene. Our data are also consistent with $^{40}Ar/^{39}Ar$ and (U-Th)/He thermochronological results from easternmost Tibet (Longmen Shan and adjacent regions) that indicate remarkably slow cooling (and inferred denudation rates of <0.1 mm/yr) from Mesozoic to late Miocene time (Kirby et al., in press). Finally, low-relief geomorphic surfaces of Miocene age in central and eastern Tibet (Shackleton and Chang, 1988; Yi et al., 2000; Kirby et al., in press) further attest to negligible Neogene erosion over much of the plateau interior.

In summary, the combination of (1) sedimentologic and compositional evidence for small-scale drainage systems, lacustrine-dominated basin sedimentation, relatively low sediment-accumulation rates, and limited erosional unroofing during Paleocene–Eocene evolution of syncontractional basins (this study) and (2) thermochronologic and geomorphic evidence for limited denudation (e.g., Shackleton and Chang, 1988; Yi et al., 2000; Kirby et al., 2002) suggests that the early Tertiary geomorphic conditions in eastern Tibet were similar to modern conditions (i.e., internal drainage, low relief, low denudation) across much of the interior of the Tibetan plateau.

CONCLUSIONS

1. Paleocene–Eocene basin development in the Nangqian-Yushu region of east-central Tibet was produced by northeast-southwest contraction during the initial stage of the India-Asia collision. Growth strata in both fine- and coarse-grained successions indicate sedimentation synchronous with fold-thrust deformation. The limited width (<15 km), thickness (<2 km), and areal extent (generally <10^3 km^2) of the basins suggest that their formation was controlled by closely spaced, thin-skinned thrusts that sole into a common décollement at ~5 km depth. Syncontractional basin development terminated by Oligocene time, prior to the onset of right-slip faulting that persisted into Neogene and possibly Quaternary time.

2. Facies analysis and provenance data indicate that the basins of the Nangqian-Yushu region evolved as lacustrine-dominated depositional systems in disconnected, internally drained basins separated by fold-thrust structures developed in Carboniferous–Triassic rocks. Each basin was the site of mud and carbonate deposition in offshore to nearshore lacustrine settings and gravel and sand deposition in fan-delta to alluvial-fan environments. Similar depositional conditions may

have characterized other Tertiary basins in the interior of the Tibetan plateau.

3. Although a middle Cretaceous section is present locally at the base of the Nangqian basin, most sediment accumulation and syndepositional contraction occurred during Paleocene through middle Eocene time. An approximate middle Cretaceous age for organic-rich mudstone in the lowermost fill of the Nangqian basin is based on palynomorph and ostracod assemblages. Paleocene–Eocene deposition in all four basins is supported by mollusks, palynomorphs, and plant fossils of Paleogene age as well as 51–49 Ma $^{40}Ar/^{39}Ar$ ages from igneous rocks that intrude and unconformably overlie the Shanglaxiu basin. Late-stage deposition during late middle Eocene time is supported by 38–37 Ma $^{40}Ar/^{39}Ar$ ages from interbedded volcanic rocks in uppermost fill of the Nangqian basin.

4. A predominance of fine-grained lacustrine facies, a provenance history suggesting limited unroofing, and relatively low average rates of sediment accumulation are compatible with small drainage networks (<10^3 km^2), short main-stem rivers (<50 km long), shallow regional slopes, and minimal local relief in the Nangqian-Yushu region during early Tertiary time. These geomorphic conditions are similar to the modern internally drained, low-relief part of the Tibetan plateau, suggesting that the deeply incised rivers of eastern Tibet, particularly the Mekong and Yangtze Rivers, postdate Paleogene basin development.

REFERENCES CITED

Allègre, C.J., Courtillot, V., Tapponnier, P., Hirn, A., Mattauer, M., Coulon, C., Jaeger, J.J., Achache, J., Schaerer, U., Marcoux, J., Burg, J.P., Girardeau, J., Armijo, R., Gariepy, C., Goepel, C., Li, T., Xiao, X., Chang, C., Li, G., Lin, B., Teng, J., Wang, N., Chen, G., Han, T., Wang, X.., Den, W., Sheng, H., Cao, Y., Zhou, J., Qiu, H., Bao, P., Wang, S., Wang, B., Zhou, Y., and Xu, R., 1984, Structure and evolution of the Himalaya-Tibet orogenic belt: Nature, v. 307, p. 17–22.

Armijo, R., Tapponnier, P., and Han, T., 1989, Late Ceno-

zoic right-lateral strike-slip faulting in southern Tibet: Journal of Geophysical Research, v. 94, p. 2787–2838.

Ashley, G.M., 1975, Rhythmic sedimentation in glacial Lake Hitchcock, Massachusetts-Connecticut, in Jopling, A.V., and McDonald, B.C., eds., Glaciofluvial and glaciolacustrine sedimentation: Society of Economic Paleontologists and Mineralogists Special Publication 23, p. 304–320.

Bally, A.W., Chou, I.M., Clayton, R., Eugster, H.P., Kidwell, S., Meckel, L.D., Ryder, R.T., Watts, A.B., and Wilson, A.A., 1986, Notes on sedimentary basins in China: Report of the American Sedimentary Basins Delegation to the People's Republic of China: U.S. Geological Survey Open-File Report 86-237, 108 p.

Blair, T.C., and McPherson, J.G., 1994, Alluvial fans and their natural distinction from rivers based on morphology, hydraulic processes, sedimentary processes, and facies assemblages: Journal of Sedimentary Research, v. A64, p. 450–489.

Brookfield, M.E., 1998, The evolution of the great river systems of southern Asia during the Cenozoic India-Asia collision: Rivers draining southwards: Geomorphology, v. 22, p. 285–312.

Burbank, D.W., Beck, R.A., and Mulder, T., 1996, The Himalayan foreland basin, in Yin, A., and Harrison, T.M., eds., The tectonic evolution of Asia: New York, Cambridge University Press, p. 149–189.

Burchfiel, B.C., Chen, Z., Liu, Y., and Royden, L.H., 1995, Tectonics of the Longmen Shan and adjacent regions, central China: International Geology Review, v. 37, p. 661–735.

Burg, J.P., and Chen, G.M., 1984, Tectonics and structural zonation of southern Tibet, China: Nature, v. 311, p. 219–223.

Burke, K., and Lucas, L., 1989, Thrusting on the Tibetan plateau within the last 5 Ma, in Şengör A.M.C., ed., Tectonic evolution of the Tethyan region: Boston, Kluwer Academic Publishers, p. 507–512.

Chen, S.F., Wilson, C.J.L., and Worley, B.A., 1995, Tectonic transition from the Songpan-Garzê fold belt to the Sichuan Basin, south-western China: Basin Research, v. 7, p. 235–253.

DeCelles, P.G., Gray, M.B., Ridgway, K.D., Cole, R.B., Srivastava, P., Pequera, N., and Pivnik, D.A., 1991, Kinematic history of a foreland uplift from Paleocene synorogenic conglomerate, Beartooth Range, Wyoming and Montana: Geological Society of America Bulletin, v. 103, p. 1458–1475.

DeCelles, P.G., Gehrels, G.E., Quade, J., Ojha, T.P., Kapp, P.A., and Upreti, B.N., 1998, Neogene foreland basin deposits, erosional unroofing, and the kinematic history of the Himalayan fold-thrust belt, western Nepal: Geological Society of America Bulletin, v. 110, p. 2–21.

DeCelles, P.G., Gehrels, G.E., Quade, J., LaReau, B., and Spurlin, M., 2000, Tectonic implications of U-Pb zircon ages of the Himalayan orogenic belt in Nepal: Science, v. 288, p. 497–499.

Dewey, J.F., Shackleton, R.M., Chang, C., and Sun, Y., 1988, The tectonic evolution of the Tibetan plateau: Philosophical Transactions of the Royal Society of London, v. A327, p. 379–413.

Einsele, G., and Hinderer, M., 1998, Quantifying denudation and sediment-accumulation systems (open and closed lakes): Basic concepts and first results: Palaeogeography, Palaeoclimatology, Palaeoecology, v. 140, p. 7–21.

Graham, S.A., Hendrix, M.S., Wang, L.B., and Carroll, A.R., 1993, Collisional successor basins of western China: Impact of tectonic inheritance on sand composition: Geological Society of America Bulletin, v. 105, p. 323–344.

Hack, J.T., 1957, Studies of longitudinal stream profiles in Virginia and Maryland: U.S. Geological Survey Professional Paper 294-B, 97 p.

Hallet, B., and Molnar, P., 2001, Distorted drainage basins as markers of crustal strain east of the Himalaya: Journal of Geophysical Research, v. 106, p. 13697–13709.

Hardie, L.A., Smoot, J.P., and Eugster, H.P., 1978, Saline lakes and their deposits: A sedimentological approach, in Matter, A., and Tucker, M.E., eds., Modern and an-

cient lake sediments: International Association of Sedimentologists Special Publication 2, p. 7–41.

Harris, N.B.W., Xu, R., Lewis, C.L., Hawkesworth, C.J., and Zhang, Y., 1988, Isotope geochemistry of the 1985 Tibet Geotraverse, Lhasa to Golmud: Philosophical Transactions of the Royal Society of London, v. A327, p. 263–285.

Heller, P.L., Angevine, C.L., Winslow, N.S., and Paola, C., 1988, Two-phase stratigraphic model of foreland-basin sequences: Geology, v. 16, p. 501–504.

Horton, B.K., 1998, Sediment accumulation on top of the Andean orogenic wedge: Oligocene to late Miocene basins of the Eastern Cordillera, southern Bolivia: Geological Society of America Bulletin, v. 110, p. 1174–1192.

Horton, B.K., and DeCelles, P.G., 2001, Modern and ancient fluvial megafans in the foreland basin system of the central Andes, southern Bolivia: Implications for drainage network evolution in fold-thrust belts: Basin Research, v. 13, p. 43–63.

Horton, B.K., and Schmitt, J.G., 1996, Sedimentology of a lacustrine fan-delta system, Miocene Horse Camp Formation, Nevada, USA: Sedimentology, v. 43, p. 133–155.

Huang, K., Opdyke, N.D., Li, J., and Peng, X., 1992, Paleomagnetism of Cretaceous rocks from eastern Qiangtang terrane of Tibet: Journal of Geophysical Research, v. 97, p. 1789–1799.

Huo, Y.L., and Tan, S.D., 1995, Exploration case history and petroleum geology in Jiuquan continental basin: Beijing, Petroleum Industry Press, 211 p.

Kapp, P.A., Yin, A., Manning, C., Murphy, M.A., and Harrison, T.M., 1999, Post-mid-Cretaceous shortening along the Banggong-Nujiang suture and in west-central Qiangtang, Tibet [abs.]: Eos (Transactions, American Geophysical Union), v. 79, p. 794.

Kapp, P., Yin, A., Manning, C., Murphy, M.A., Harrison, T.M., Ding, L., Deng, X., and Wu, C.-M., 2000, Blueschist-bearing metamorphic core complexes in the Qiangtang block reveal deep crustal structure of northern Tibet: Geology, v. 28, p. 19–22.

Kelts, K., and Hsü, K.J., 1978, Fresh water carbonate sedimentation, in Lerman, A., ed., Lakes: Chemistry, geology, physics: Berlin, Springer-Verlag, p. 295–323.

Kirby, E., Reiners, P.W., Krol, M.A., Whipple, K.X, Hodges, K.V., Farley, K.A., Tang, W., and Chen, Z., in press, Late Cenozoic evolution of the eastern margin of the Tibetan plateau: Inferences from ^{40}Ar/^{39}Ar and (U-Th)/He thermochronology: Tectonics.

Lawton, T.F., Roca, E., and Guimerà, J., 1999, Kinematic-stratigraphic evolution of a growth syncline and its implications for tectonic development of the proximal foreland basin, southeastern Ebro basin, Catalunya, Spain: Geological Society of America Bulletin, v. 111, p. 412–431.

Leeder, M.R., Smith, A.B., and Yin, J., 1988, Sedimentology, palaeoecology and palaeoenvironmental evolution of the 1985 Lhasa to Golmud Geotraverse: Philosophical Transactions of the Royal Society of London, v. A327, p. 107–143.

Leloup, P.H., Lacassin, R., Tapponnier, R., Zhong, D., Lui, X., Zhang, L., and Ji, S. 1995, Kinematics of Tertiary left-lateral shearing at the lithospheric-scale in the Ailao Shan–Red River shear zone (Yunnan, China): Tectonophysics, v. 251, p. 3–84.

Li, Y., 1988, The application of Ostracoda to the location of the nonmarine Jurassic-Cretaceous boundary in the Sichuan Basin of China, in Hanai, T., Ikeya, N., and Ishizaki, K., eds., Evolutionary biology of Ostracoda: Amsterdam-Tokyo, Elsevier-Kodansha, p. 1245–1260.

Li, Y., and Yang, F., 1983, Late Jurassic fresh-water ostracods from the Qaidam Basin: Bulletin of the Chengdu Institute of Geology and Mineral Resources, Chinese Academy of Geological Sciences, v. 7, p. 77–83 (in Chinese).

Link, M.H., and Osborne, R.H., 1978, Lacustrine facies in the Pliocene Ridge Basin Group: Ridge basin, California, in Matter, A., and Tucker, M.E., eds., Modern and ancient lake sediments: International Association of Sedimentologists Special Publication 2, p. 169–187.

Liu, Z.Q., compiler, 1988, Geological map of Qinghai-Xizang (Tibet) plateau and adjacent areas (1:1,500,000 scale): Beijing, Geologic Publishing House, Chengdu Institute of Geology and Mineral Resources, Chinese Academy of Geological Sciences.

Liu, Z., and Wang, C., 2001, Facies analysis and depositional systems of Cenozoic sediments in the Hoh Xil basin, northern Tibet: Sedimentary Geology, v. 140, p. 251–270.

Liu, Z, Wang, C., and Yi, H., 2001, Evolution and mass accumulation of the Cenozoic Hoh Xil basin, northern Tibet: Journal of Sedimentary Research, v. 71, p. 971–984.

Metcalfe, I., 1996, Gondwanaland dispersion, Asian accretion and evolution of eastern Tethys: Australian Journal of Earth Sciences, v. 43, p. 605–623.

Métivier, F., Gaudemer, Y., Tapponnier, P., and Meyer, B., 1998, Northeastward growth of the Tibet plateau deduced from balanced reconstruction of two depositional areas: The Qaidam and Hexi Corridor basins, China: Tectonics, v. 17, p. 823–842.

Métivier, F., Gaudemer, Y., Tapponnier, P., and Klein, M., 1999, Mass accumulation rates in Asia during the Cenozoic: Geophysical Journal International, v. 137, p. 280–318.

Meyer, B., Tapponnier, P., Bourjot, L., Métivier, F., Gaudemer, Y., Peltzer, G., Guo, S., and Chen, Z., 1998, Crustal thickening in Gansu-Qinghai, lithospheric mantle subduction, and oblique, strike-slip controlled growth of the Tibet plateau: Geophysical Journal International, v. 135, p. 1–47.

Meyerhoff, A.A., Kamen-Kaye, M., Chen, C., and Taner, I., 1991, China: Stratigraphy, paleogeography and tectonics: Boston, Kluwer Academic Publishers, 188 p.

Montgomery, D.R., and Dietrich, W.E., 1992, Channel initiation and the problem of landscape scale: Science, v. 255, p. 826–830.

Murphy, M.A., Yin, A., Harrison, T.M., Durr, S.B., Chen, Z., Ryerson, F.J., Kidd, W.S.F., Wang, X., and Zhou, X., 1997, Did the Indo-Asian collision alone create the Tibetan plateau?: Geology, v. 25, p. 719–722.

Nemec, W., and Postma, G., 1993, Quaternary alluvial fans in southwestern Crete: Sedimentation processes and geomorphic evolution, in Marzo, M., and Puigdefábregas, C., eds., Alluvial sedimentation: International Association of Sedimentologists Special Publication 17, p. 235–276.

Nemec, W., and Steel, R.J., 1988, What is a fan delta and how do we recognize it?, in Nemec, W., and Steel, R.J., eds., Fan deltas: Sedimentology and tectonic settings: London, Blackie and Son, p. 3–13.

Nie, S., Yin, A., Rowley, D., and Jin, Y., 1994, Exhumation of the Dabie Shan ultrahigh-pressure rocks and accumulation of the Songpan-Ganzi flysch sequence, central China: Geology, v. 22, p. 999–1002.

Ori, G.G., and Friend, P.F., 1986, Sedimentary basins formed and carried piggyback on active thrust sheets: Geology, v. 12, p. 475–478.

Pang, Q., and Whatley, R., 1990, The biostratigraphical sequence of Mesozoic nonmarine ostracod assemblages in northern China, in Whatley, R., and Maybury, C., eds., Ostracoda and global events: London, Chapman and Hall, p. 239–250.

Peltzer, G., and Tapponnier, P., 1988, Formation and evolution of strike-slip faults, rifts and basins during the India-Asia collision: An experimental approach: Journal of Geophysical Research, v. 93, p. 15 085–15 117.

Postma, G., 1983, Water escape structures in the context of a depositional model of a mass flow dominated conglomeratic fan-delta (Abrioja Formation, Pliocene, Almeria basin, southeast Spain): Sedimentology, v. 30, p. 91–103.

Qinghai BGMR [Qinghai Bureau of Geology and Mineral Resources], 1983a, Geologic map of the Nangqian region, with geologic report (1:200 000 scale): Unpublished, 198 p.

Qinghai BGMR [Qinghai Bureau of Geology and Mineral Resources], 1983b, Geologic map of the Shanglaxiu region, with geologic report (1:200 000 scale): Unpublished, 220 p.

Qinghai BGMR [Qinghai Bureau of Geology and Mineral Resources], 1991, Regional geology of Qinghai province: Beijing, Geological Publishing House, 662 p.

Ratschbacher, L., Frisch, W., Liu, G., and Chen, C., 1994, Distributed deformation in southern and western Tibet during and after the India-Asia collision: Journal of Geophysical Research, v. 99, p. 19917–19945.

Ratschbacher, L., Frisch, W., Chen, C., and Pan, G., 1996, Cenozoic deformation, rotation, and stress patterns in eastern Tibet and western Sichuan, China, in Yin, A., and Harrison, T.M., eds., The tectonic evolution of Asia: New York, Cambridge University Press, p. 227–249.

Riba, O., 1976, Syntectonic unconformities of the Alto Cardener, Spanish Pyrenees: A genetic interpretation: Sedimentary Geology, v. 15, p. 213–233.

Ridgway, K.D., and DeCelles, P.G., 1993, Stream-dominated alluvial fan and lacustrine depositional systems in Cenozoic strike-slip basins, Denali fault system, Yukon Territory, Canada: Sedimentology, v. 40, p. 645–666.

Royden, L.H., Burchfiel, B.C., King, R.W., Wang, E., Chen, Z., Shen, F., and Liu, Y., 1997, Surface deformation and lower crustal flow in eastern Tibet: Science, v. 276, p. 788–790.

Şengör, A.M.C., and Natal'in, B.A., 1996, Paleotectonics of Asia: Fragments of a synthesis, in Yin, A., and Harrison, T.M., eds., The tectonic evolution of Asia: New York, Cambridge University Press, p. 486–640.

Shackleton, R.M., and Chang, C., 1988, Cenozoic uplift and deformation of the Tibetan plateau: The geomorphological evidence: Philosophical Transactions of the Royal Society of London, v. A327, p. 365–377.

Smith, G.A., 1986, Coarse-grained nonmarine volcaniclastic sediment: Terminology and depositional process: Geological Society of America Bulletin, v. 97, p. 1–10.

Sobel, E.R., and Dumitru, T.A., 1997, Thrusting and exhumation around the margins of the western Tarim Basin during the India-Asia collision: Journal of Geophysical Research, v. 102, p. 5043–5063.

Song, T., and Wang, X., 1993, Structural styles and stratigraphic patterns of syndepositional faults in a contractional setting: Examples from Quaidam Basin, northwestern China: American Association of Petroleum Geologists Bulletin, v. 77, p. 102–117.

Spurlin, M., Yin, A., Harrison, T.M., Horton, B.K., Zhou, J., and Wang, J., 2000, Two phases of Cenozoic deformation in east-central Tibet: Thrusting followed by right-slip faulting [abs.]: Eos (Transactions, American Geophysical Union), v. 81, p. 1092.

Sturm, M., and Matter, A., 1978, Turbidites and varves in Lake Brienz (Switzerland): Deposition of clastic detritus by density currents, in Matter, A., and Tucker, M.E., eds., Modern and ancient lake sediments: International Association of Sedimentologists Special Publication 2, p. 147–168.

Su, D., Li, Y., Yu, J., Zhang, W., Zhang, L., Pu, R., and Yang, R., 1983, Late Mesozoic biostratigraphy of nonmarine Ostracoda and pollen and spores in China: Acta Geologica Sinica, v. 57, p. 329–346 (in Chinese with English abstract).

Surdam, R.C., and Stanley, K.O., 1979, Lacustrine sedimentation during the culminating phase of Eocene Lake Gosiute, Wyoming (Green River Formation): Geological Society of America Bulletin, v. 90, p. 93–110.

Talling, P.J., Lawton, T.F., Burbank, D.W., and Hobbs, R.S., 1995, Evolution of latest Cretaceous–Eocene nonmarine deposystems in the Axhandle piggyback basin of central Utah: Geological Society of America Bulletin, v. 107, p. 297–315.

Van der Woerd, J., Ryerson, F.J., Tapponnier, P., Meriaux, A.-S., Gaudemer, Y., Meyer, B., Finkel, R.C., Caffee, M.W., Zhao, G., and Xu, Z., 2000, Uniform slip-rate along the Kunlun fault: Implications for seismic behaviour and large-scale tectonics: Geophysical Research Letters, v. 27, p. 2353–2356.

Wang, Z., compiler, 1995, Atlas of the sedimentary facies and palaeogeography of Yunnan: Kunming, China, Yunnan Science and Technology Press, Yunnan Bureau of Geology and Mineral Resources, 228 p.

Wang, E., and Burchfiel, B.C., 2000, Late Cenozoic to Holocene deformation in southwestern Sichuan and adjacent Yunnan, China, and its role in formation of the southeastern part of the Tibetan plateau: Geological Society of America Bulletin, v. 112, p. 413–423.
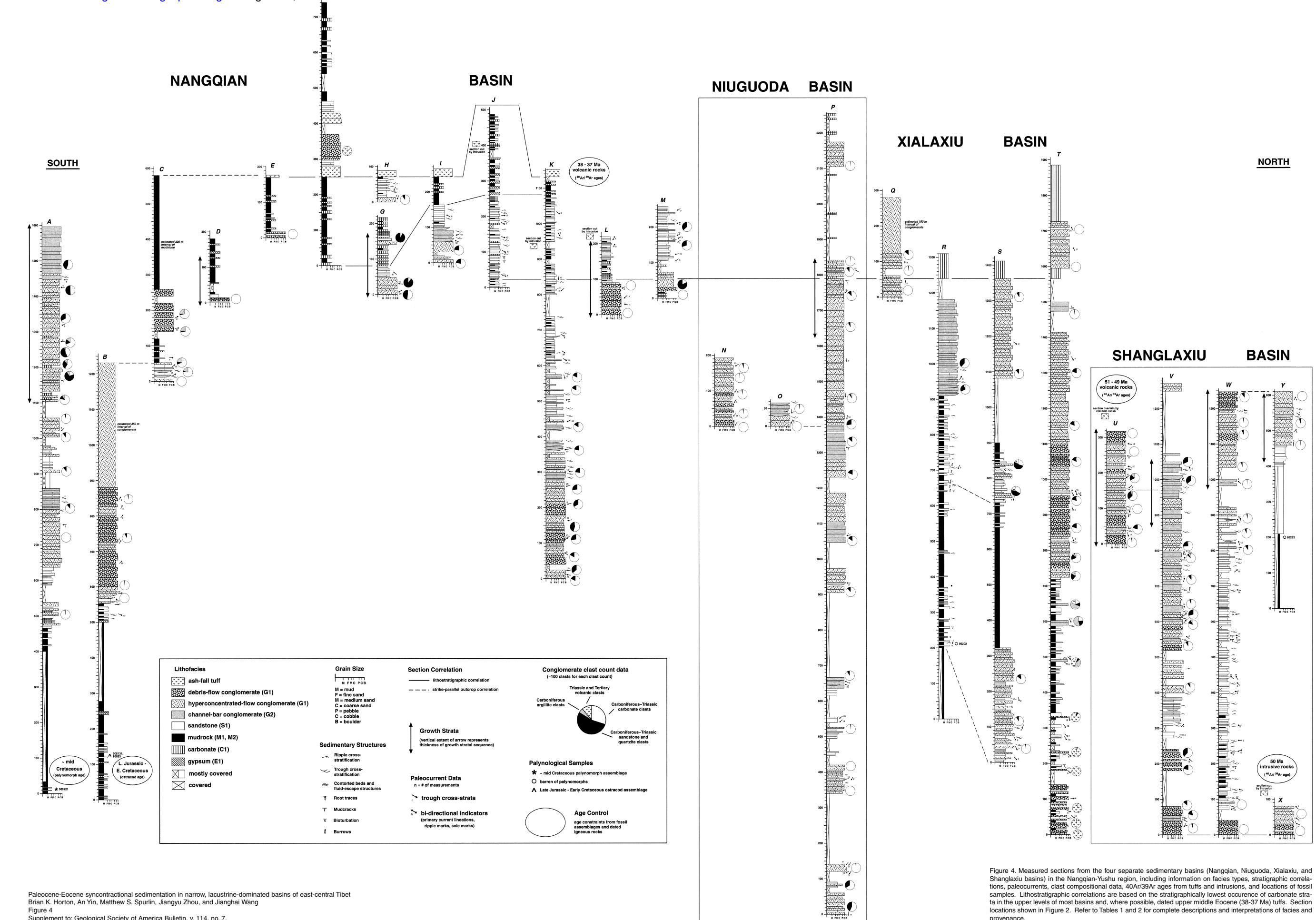
Wang, J.H., Yin, A., Harrison, T.M., Grove, M., Zhang, Y.Q., and Xie, G.H., 2001, A tectonic model for Cenozoic igneous activities in the eastern Indo-Asian collision zone: Earth and Planetary Science Letters, v. 188, p. 123–133.

Weirich, F.H., 1986, The record of density-influenced underflows in a glacial lake: Sedimentology, v. 33, p. 261–277.

Xu, G., and Kamp, P.J.J., 2000, Tectonics and denudation adjacent to the Xianshuihe fault, eastern Tibetan plateau: Constraints from fission track thermochronology: Journal of Geophysical Research, v. 105, p. 19 231–19 251.

Yi, H., Wang, C., Liu, S., Liu, Z., and Wang, S., 2000, Sedimentary record of the planation surface in the Hoh Xil region of the northern Tibetan plateau: Acta Geologica Sinica, v. 74, p. 827–835.

Yin, A., and Harrison, T.M., 2000, Geologic evolution of the Himalayan-Tibetan orogen: Annual Review of Earth and Planetary Sciences, v. 28, p. 211–280.

Yin, A., and Nie, S., 1996, A Phanerozoic palinspastic reconstruction of China and its neighboring regions, in Yin, A., and Harrison, T.M., eds., The tectonic evolution of Asia: New York, Cambridge University Press, p. 18–35.

Yin, A., Harrison, T.M., Ryerson, F.J., Chen, W., Kidd, W.S.F., and Copeland, P., 1994, Tertiary structural evolution of the Gangdese thrust system, southeastern Tibet: Journal of Geophysical Research: v. 99, p. 18 175–18 201.

Yin, A., Harrison, T.M., Murphy, M.A., Grove, M., Nie, S., Ryerson, F.J., Wang, X.F., and Chen, Z.L., 1999, Tertiary deformation history of southeastern and southwestern Tibet during the Indo-Asian collision: Geological Society of America Bulletin, v. 111, p. 1644–1664.

Zeitler, P.K., Meltzer, A.S., Koons, P.O., Craw, D., Hallet, B., Chamberlain, C.P., Kidd, W.S.F., Park, S.K., Seeber, L., Bishop, M., and Shroder, J., 2001, Erosion, Himalayan geodynamics, and the geomorphology of metamorphism: GSA Today, v. 11, no. 1, p. 4–9.

Zhou, D., and Graham, S.A., 1996, The Songpan-Ganzi complex of the West Qinling Shan as a Triassic remnant ocean basin, in Yin, A., and Harrison, T.M., eds., The tectonics of Asia: New York, Cambridge University Press, p. 281–299.

Figure 4. Measured sections from the four separate sedimentary basins (Nangqian, Niuguoda, Xialaxiu, and Shanglaxiu basins) in the Nangqian-Yushu region, including information on facies types, stratigraphic correlations, paleocurrents, clast compositional data, 40Ar/39Ar ages from tuffs and intrusions, and locations of fossil samples. Lithostratigraphic correlations are based on the stratigraphically lowest occurrence of carbonate strata in the upper levels of most basins and, where possible, dated upper middle Eocene (38-37 Ma) tuffs. Section locations shown in Figure 2. Refer to Tables 1 and 2 for complete descriptions and interpretations of facies and provenance.

Paleocene-Eocene syncontractional sedimentation in narrow, lacustrine-dominated basins of east-central Tibet
Brian K. Horton, An Yin, Matthew S. Spurlin, Jiangyu Zhou, and Jianghai Wang
Figure 4
Supplement to: Geological Society of America Bulletin, v. 114, no. 7.